HHS Public Access

Author manuscript

Nano Res. Author manuscript; available in PMC 2015 October 23.

Published in final edited form as:

Nano Res. 2014 October ; 7(10): 1381–1403. doi:10.1007/s12274-014-0507-y.

Glyconanomaterials: Emerging applications in biomedical research

Xuan Chen[1], **Olof Ramström**[2], and **Mingdi Yan**[1,2]

Mingdi Yan: mingdi_yan@uml.edu

[1]Department of Chemistry, University of Massachusetts Lowell, Lowell, MA 01854, USA

[2]Department of Chemistry, KTH—Royal Institute of Technology, Stockholm S-10044, Sweden

Abstract

Carbohydrates constitute the most abundant organic matter in nature, serving as structural components and energy sources, and mediating a wide range of cellular activities. The emergence of nanomaterials with distinct optical, magnetic, and electronic properties has witnessed a rapid adoption of these materials for biomedical research and applications. Nanomaterials of various shapes and sizes having large specific surface areas can be used as multivalent scaffolds to present carbohydrate ligands. The resulting glyconanomaterials effectively amplify the glycan-mediated interactions, making it possible to use these materials for sensing, imaging, diagnosis, and therapy. In this review, we summarize the synthetic strategies for the preparation of various glyconanomaterials. Examples are given where these glyconanomaterials have been used in sensing and differentiation of proteins and cells, as well as in imaging glycan-medicated cellular responses.

Keywords

glyconanomaterials; carbohydrates; imaging; therapy

1 Introduction

Carbohydrates represent one of the major components in all living systems and also constitute the most abundant organic matter in nature. Although there are only a limited number of monosaccharide structures, these simple carbohydrates, through different regioand stereochemical linkages, can produce a large number of disaccharides, oligosaccharides and polysaccharides having diverse structures, compositions, and stereochemistry. It is therefore of no surprise that carbohydrates play important roles in various aspects of life and nature. For instance, cellulose, the structural component in plant cell walls, is the main component of wood and cotton that have served to protect human for centuries. Also critical to the development of human lives and civilization is starch, another polysaccharide found in large amounts in primary staple foods including rice, wheat, corn and potatoes. Glycan structures, primarily oligosaccharides, are present on the surface of mammalian and bacteria cells, as well as viruses. Through carbohydrate–carbohydrate and

Correspondence to: Mingdi Yan, mingdi_yan@uml.edu.

carbohydrate–lectin interactions, these entities are involved in a wide range of cellular activities, including cell–cell communication [1–3], immune response [4], and bacterial and viral infections [5]. For instance, the HIV virus gains entry into cells by attaching its envelope glycoprotein gp120 to immune cell surface receptor CD4 [6]. Successful sea urchin fertilization relies on sperm-egg adhesion mediated by the interaction between lectins on the sperm surface and carbohydrates on the egg membrane [7]. Also, one of the key steps of cancer hematogenous metastasis depends on the adhesion of sialyl Lewis A and sialyl Lewis X (sLe^x) tetrasaccharides on human cancer cells to E-selectin expressed on vascular endothelial cells [8, 9]. Thus, studying glycan-mediated processes will not only gain fundamental understanding of these structures, but also provide insights and guidance on the design and development of effective diagnosis and therapeutic tools leading to the treatments of many diseases such as infection and cancer.

The advance of glycoscience has however been hampered by a number of challenges. These include the difficulties to achieve controlled synthesis of oligosaccharides with well-defined structures, and the relatively low affinities of carbohydrate–lectin interactions in comparison to counterparts involving other biological species such as enzymes and antibodies. The latter of these may be addressed using glyconanomaterials, providing unique platforms where the nanomaterial may serve as a cell mimic to present carbohydrate molecules. The high specific surface area allows the nanomaterial to accommodate high-density carbohydrate ligands, enhancing carbohydrate-mediated interactions by way of multivalency. We [10–15] and others [16, 17] have thus shown that the affinities of glyconanomaterials with lectins are several orders of magnitude higher than those of free ligands. Furthermore, by conjugating epitopes of more complex glycans on nanoparticles, the affinities of the resulting nanomaterials could surpass those of the original oligosaccharide glycans [12, 18, 19]. These studies have shown that glyconanomaterials can be used as tools to study carbohydrate-mediated interactions. These investigations have demonstrated the potential of glyconanomaterials in diagnosis and treatment of diseases. Glyconanomaterials present additional values in terms of structural diversity. The research field is thus largely fueled by the rapid advances in nanotechnology, where nanomaterials of different composition, size, shape, chemical and physical properties are being developed. The availability of these materials has enabled the study of how glycan-mediated cellular interactions and responses can be modulated by parameters such as ligand density, size, and shape [11]. Imaging and diagnosis applications also become possible when the nanomaterials possess optical, magnetic, and electronic properties that allow the transduction of cellular interactions into readable signals. Furthermore, when nanomaterials are used as carriers, therapeutics can be developed with the aid of carbohydrate ligands to facilitate the treatment of diseases.

In this review, we will give an overview of preparation methods of glyconanomaterials, and their applications in sensing, imaging, diagnosis, and therapeutics. We will focus on carbon nanomaterials, metal nanoparticles, quantum dots (QDs), magnetic nanoparticles (MNPs) and silica nanoparticles (SNPs). Glyconanomaterials based on molecular scaffolds of polymers, dendrimers, lipids, micelles, etc. have a long history, and are well documented in the literature. Readers are referred to the cited reviews to learn more about glycopolymers [20–24], glycodendrimers [25–28], and glycoliposomes [29–31]. Besides oligosaccharides, which constitutes the main focus of the present review, polysaccharides such as cellulose,

dextran, chitosan, glycosaminoglycans (GAGs), represent another important class of carbohydrates. These biocompatible polysaccharides can provide a protection layer to reduce the cytotoxicity of encapsulated nanoparticles such as QDs and graphene oxide. The polysaccharide coating can also help prolong the circulation time of nanomateirals. Furthermore, the abundant reactive groups on polysaccharides can be used to conjugate additional moieties to provide functions such as cell-specific targeting and responsiveness towards external stimuli. For this topic, we direct readers to reviews in references [32–35] for detailed discussions.

2 Preparation of glyconanomaterials

2.1 Carbon nanomaterials

Carbon-based nanomaterials have a long history, from the oldest nanomaterial of amorphous carbon, to the newly discovered fullerenes, carbon nanotubes (CNTs) and graphene. These materials continue to break records of material and physical properties, and hold promise to impact a wide range of fields, including electronics, sensing, imaging and therapeutics. However, several disadvantages limit their biological applications, such as poor water solubility, lack of reactive functionality, and potentially high cytotoxicity [36]. An effective way to overcome these limitations is to introduce an organic coating on the carbon materials. Carbohydrates are in this sense suitable candidates that not only increase the biocompatibility and solubility, but also introduce molecular recognition features to the carbon materials, which can impact cellular interactions and uptake of these entities.

One approach to carbohydrate conjugation is through non-covalent interactions between carbon materials and modified carbohydrates. In this case, carbohydrates are chemically derivatized with nonpolar moieties such as lipids [37–41], polyaromatic hydrocarbons [42–44], or porphyrins [45], which are capable of interacting with the hydrophobic carbon materials (Fig. 1). The resulting carbon materials are not chemically functionalized, and their properties are thus preserved. For example, Bertozzi and co-workers coated single-wall CNTs (SWCNTs) with poly(methyl vinyl ketone) having a C_{18} lipid tail that could self-assemble on the SWCNTs through hydrophobic effects (Fig. 1(a)) [37]. The polymer was functionalized with α-D-*N*-acetylgalactosamine (α-GalNAc) as pendant groups. The resulting mucin mimic-modified SWCNTs resisted non-specific protein adsorption, and could also recognize the *Helix pomatia* agglutinin (HPA), an α-GalNAc-binding lectin. In another study, the group functionalized monosaccharides with pyrene, which were subsequently adsorbed on SWCNTs (Fig. 1(b)) [43]. The modified SWCNTs were used to promote cell adhesion and study dynamic cellular activities. The same concept was used in a work by Lin et al. where pristine graphene was functionalized with pyrenemodified maltose [44]. Upon adsorption, graphene quenched the pyrene fluorescence, which was then recovered by addition of the lectin Concanavalin A (Con A). This displacement-type assay provided a means for lectin sensing, where the detection limit was estimated to be 0.8 nM in the case of Con A.

Covalent modification requires a chemical reaction between the carbon nanomaterial and the carbohydrate. In this case, either the carbon nanomaterial or the carbohydrate, or both, need to be chemically functionalized (Fig. 2). Carbon nanomaterials are relatively inert

chemically, and therefore, methods for the chemical functionalization of carbon materials often involve the use of reactive intermediates such as azomethine ylides, radicals, carbenes, and nitrenes [46–48]. Among the carbon materials, fullerenes, especially buckminsterfullerene C_{60}, have the richest and the most established functionalization chemistry. Well-defined fullerene derivatives can be synthesized, and the number of functional groups can be precisely controlled [49, 50].

For CNTs and graphene, the most common way to achieve covalent functionalization is to use the oxidized forms. Oxidation generates oxygen-containing functional groups, such as epoxy and carboxylic acid moieties, which can then be used to react with, e.g., amine-functionalized carbohydrates [51, 52]. In the case of graphene, the vast majority of the reported methods uses the oxidized form, which can be prepared inexpensively from graphite to produce single-layer graphene oxide in large quantities. Single-layer pristine graphene, on the other hand, is still difficult to obtain, especially on a larger scale.

Aryl diazonium salts are among the most used reagents to functionalize pristine CNTs and graphene. The reaction has been suggested to proceed via aryl radicals that are generated by electron transfer from the CNTs or graphene to the aryl diazonium ions after elimination of N_2 [53]. This chemistry was for example used by Torres et al., who prepared SWCNTs and graphene coated with α-D-mannosyl (Man) dendrons following a sequential functionalization approach [54]. A diazonium salt, prepared from 4-[(trimethylsilyl)ethynyl)]aniline with isoamyl nitrite, was activated under microwave irradiation and reacted with SWCNTs and graphene. The carbohydrates were subsequently conjugated to the material via a copper-catalyzed alkyne-azide cycloaddition (CuAAC) reaction using azide-functionalized α-D-mannosyl dendrons (Fig. 2(a)).

Another useful functionalization method relies on azomethine ylides, which undergo 1,3-dipolar cycloaddition with CNTs to form pyrrolidine derivatives (Fig. 2(b)). This method can also be applied to indirect carbohydrate functionalization as exemplified in a study by Hong et al. The azomethine ylides were in this case generated from α-amino acids and an aldehyde, and carboxy-functionalized D-*N*-acetylglucosamine (GlcNAc) structures were then conjugated to the resulting pyrrolidinyl CNTs (Fig. 2(b)) [55].

Nitrenes constitute another widely used reactive intermediate to introduce functional groups directly on pristine carbon nanomaterials. Generated by thermal or light activation, these reactive intermediates are perceived to undergo cheletropic cycloaddition reactions with alkenes to form aziridines [56, 57]. Azide-functionalized carbohydrates were used to functionalize CNTs in refluxing chlorobenzene to render CNTs water soluble (Fig. 2(c)) [58]. This chemistry is very efficient, and perfluorophenyl nitrene formation was, for example, developed in our laboratory to functionalize different pristine carbon nanomaterials (Fig. 2(d)) [48, 51, 59–63]. Unlike the singlet phenyl nitrene that primarily ring expands to form the dehydroazepine, the singlet perfluorophenyl nitrene can undergo efficient C=C addition reactions due to its longer lifetime and higher activation energy barrier for the ring expansion reaction [64–67]. Therefore, reaction with perfluorophenyl azide (PFPA) resulted in covalent functionalization of fullerenes [68], CNTs [69] and graphene [61]. The properties of the materials can be tailored by the PFPA functionality. For

instance, pristine graphene can be made soluble in water or common organic solvents [51], and CNTs can be derivatized with polymer brushes through the conjugation of an atom-transfer radical-polymerization (ATRP) initiator to PFPA [69]. Using the *N*-hydroxysuccinimide ester functionalized PFPA (PFPA-NHS) to functionalize CNTs or graphene, the material can be further conjugated with amine-functionalized carbohydrates (Fig. 2(d)). The resulting materials selectively recognized carbohydrate-binding lectins [70].

2.2 Metal nanoparticles

Metal nanoparticles, for example Au, Ag, and Cu nanoparticles, show distinct optical properties that are different from bulk materials due to the quantum confinement effect resulting from the reduction of the particle size. The collective oscillation of electrons in the metal nanoparticles, generated by light illumination, is highly sensitive to the dielectric environment close to the nanoparticle surface. The so-called localized surface plasmon resonance (LSPR), provides a powerful means to monitor the molecular events occurring at the particle surface [71]. Many studies have taken advantage of the change in LSPR, often resulting in a color change visible by naked eyes, as a means to study carbohydrate-mediated interactions or as a detection mechanism for sensing carbohydrates [72–75]. We employed carbohydrate-conjugated Au nanoparticles (AuNPs) to differentiate plant-legume lectins [76]. Various AuNPs were treated with lectins, and changes in LSPR were subjected to linear discriminant analysis to successfully differentiate all lectins. Other studies in chemical- and bio-sensing used Au and Ag nanoparticles in surface-enhanced Raman spectroscopy (SERS) [77, 78]. For example, lactose-functionalized Ag nanoparticles were used by Graham et al. to probe the interaction with Con A, where the SERS intensity could be enhanced for lectin detection at picomolar level [77].

Among metal nanoparticles, AuNPs are most widely used due to their relative inert nature and ease of preparation in comparison to other metal nanoparticles [79]. In most cases, the carbohydrates were derivatized with a thiol or a disulfide structure, and the carbohydrate conjugation was accomplished by either a one-pot protocol or a two-step process (Fig. 3). Early examples by Penadés and coworkers demonstrated the one-pot synthetic method, where disulfide-derivatized oligosaccharides were dissolved in methanol and then mixed with an aqueous tetrachloroauric acid solution [80]. The carbohydrate-conjugated AuNPs were subsequently obtained following addition of $NaBH_4$ under vigorous stirring. Similarly, Iyer and coworkers thiolated the trisaccharide portion of globotriaosylceramide Gb3, which was then directly added into $HAuCl_4$ solution followed by $NaBH_4$ reduction [81]. The trisaccharide-conjugated AuNPs showed selective inhibition towards Shiga toxins 1 and 2. The two-step process involves the synthesis of AuNPs followed by the addition of thiolated carbohydrates. A ligand exchange reaction occurs in the second step, where the ligand, such as citric acid on the as-prepared AuNPs is replaced by the thiolated carbohydrate as a result of the higher bond strength between thiols and Au than carboxylic acid. For example, thiolated lactose and glucose derivatives prepared by Russell et al. were bound to citrate-coated AuNPs by ligand replacement [82]. Apart from these examples, a large number of other studies have involved the synthesis of Au glyconanoparticles following either of these two methods [83–87].

Post-modification of nanomaterials with carbohydrate structures is another method to conjugate carbohydrates on metal nanoparticles. In this case, a functional group is introduced on the metal nanoparticle surfaces, and carbohydrates, either derivatized or underivatized, are then conjugated to the nanoparticles through a coupling reaction. This method was, for example, used by Kataoka et al. who synthesized AuNPs with an acetal-terminated PEG-SH ligand. The acetal was then converted to the aldehyde, which in turn was used to attach *p*-aminophenyl-lactose and *p*-aminophenyl-α–D-mannose by reductive amination [88].

In a method developed in our laboratory, a two-step process was followed. AuNPs were first treated with a thiol- or disulfide-functionalized PFPA. Light activation of the PFPA then resulted in the covalent conjugation of carbohydrates to the AuNPs [11, 13, 14, 89]. In this case, the carbohydrates were used in their native form and no chemical derivatization was needed. Using this methodology, we have conjugated various carbohydrates including monosacharides, oligosaccharides and polysaccharides, as well as reducing- or non-reducing carbohydrates to AuNPs without affecting their binding affinities.

2.3 Quantum dots

QDs such as CdSe, CdTe, CdS and ZnS are crystalline semiconductor nanoparticles that display unique electronic properties resulting from the size-dependent quantum confinement. Broad absorption, tunable and narrow emission make them promising nanomaterials for imaging and sensing [90, 91]. When functionalized with carbohydrates, the water solubility and biocom-patibility of the modified QDs is enhanced, in addition to exerting molecular recognition abilities.

Similar to metal nanoparticles, carbohydrate conjugation to QDs can be accomplished by one-pot synthesis, ligand exchange reaction, or post-modification. Examples of the one-pot synthesis involved mixing disulfide-functionalized carbohydrate structures with $Cd(NO_3)_2.4H_2O$ at pH 10, followed by dropwise addition of Na_2S. As QDs were formed via the combination of Cd^{2+} and S^{2-} in basic solution, the carbohydrate disulfide ligands were directly attached to the QDs forming stabilizing layers [92, 93].

In an example of the ligand exchange protocol, Surolia and coworkers synthesized carbohydrate-conjugated CdSe–ZnS core–shell QDs by treating as-prepared QDs with thiol-functionalized lactose, melibiose and maltotriose [94]. Seeberger and coworkers further developed a controllable glyco-QDs synthesis method by using a continuous-flow microreactor. Cd and Se precursors were injected into a heating chamber followed by coating with Zn and S precursors in a second chamber. The size and fluorescence emission of the QDs could be controlled by the precursor concentrations, temperature and flow rate. Carbohydrate conjugation was accomplished in the last step in a ligand exchange chamber using thiol-functionalized carbohydrate ligands such as α-D-mannosides or β-D-galactosides [95, 96].

In the post-modification method, a functional group is introduced to QDs, which is then coupled to carbohydrates. For example, Wang and coworkers modified CdS QDs with carboxy-terminated alkylthiols, which were then used to conjugate amine-derivatized

carbohydrates using standard coupling reagents for amidation [97]. Other coupling methods such as thiolene and reductive amination have also been demonstrated to introduce carbohydrates onto QDs. For instance, Seeberger's group synthesized a series of carbohydrate-capped CdSe/ZnS core-shell QDs using the thiol-ene reaction [98]. To introduce double bonds on the nanoparticles, the QDs were first functionalized through ligand exchange with an amino-terminated PEG_{2000}-linked dihydrolipoic acid structure, followed by conjugation with a maleimide moiety. Thiol-functionalized α-D-mannosides, β-D-galactosides and β-D-galactosamine derivatives were subsequently conjugated to the QDs through a thiolene reaction. In another example, Jana et al. synthesized glyco-QDs by reductive amination [99]. The amine-functionalized QDs were prepared by encapsulating hydrophobic QDs into a polymer prepared by reverse micelle polymerization of acrylates containing *N*-(3-aminopropyl)methacrylamide. Carbohydrate immobilization was subsequently achieved by adding maltose, lactose and dextran to the amino-functionalized QDs in the presence of $Na(CN)BH_3$ at pH 9 in borate buffer followed by dialysis.

2.4 Magnetic nanoparticles

MNPs constitute an important class of nanomaterials suitable for biomedical imaging such as magnetic resonance imaging (MRI), and therapeutics such as hyperthermia treatment [100–104]. The most frequently used MNPs in these applications are iron oxide nanoparticles including magnetite (Fe_3O_4) and maghemite (γ-Fe_2O_3). Iron oxide nanoparticles can be readily prepared using simple protocols to give particles in the size range of 5–20 nm. These nano-particles can be readily dispersed in aqueous solutions to form homogeneous and stable suspensions. Iron oxide nanoparticles have excellent biocompatibility and are highly desirable for *in vivo* studies. In fact, Feraheme, a product based on carbohydrate-coated magnetite nanoparticles, have already been in clinical use for the treatment of iron deficiency anaemia [105, 106].

To prepare carbohydrate-conjugated MNPs, similar strategies to those for QDs can be adopted. For example, Horák et al. reported a one-pot protocol where D-mannose was directly added to a reaction mixture with $FeCl_3$ and $FeCl_2$ in the presence of NH_4OH [107]. In this case, D-mannose was thought to act as a metal-coordinating ligand that bound to the nanoparticles by chelation to Fe(II)/Fe(III). In this context, carboxylic acid- and phosphate-functionalized carbohydrates are also effective in binding to iron oxide nanoparticles. For example, lactobionic acid, D-gluconic acid, Ficoll and carboxy-terminated glycolipids were used by Kekkonen et al. and Baccile et al. to stabilize MNPs [108, 109]. These MNPs showed increasing stability with increasing carbohydrate ligand size. In the case of ligand exchange reactions, phosphate-functionalized, peracetylated mannose, rhamnose and ribose derivatives were used by Lartigue et al. to replace the original ligands on the iron oxide nanoparticles such as oleic acid/oleylamine. Removal of the acetyl protection groups resulted in significant increase in water solubility of the resulting nanoparticles [110].

Other routes include initial nanoparticle functionalization to introduce a functional group, followed by carbohydrate conjugation. For example, Huang and coworkers prepared magnetite nanoparticles coated with sialic acid (Sia) using amide coupling. The magnetite nanoparticles were synthesized by NH_4OH-induced co-precipitation of $FeCl_3$ and $FeSO_4$ in

the presence of dextran as a coating ligand. Amino groups were subsequently introduced by treating the dextran layer with epichlorohydrin/NaOH followed by ammonia. The partially protected sialic acid derivative having a carboxylic acid end group was then conjugated to amine-MNPs by amide coupling, and the final glyco-MNPs were obtained after removing the protecting groups in aqueous NaOH [111]. Other examples, from our group, involved the preparation of PFPA-functionalized iron oxide nanoparticles by treating the particles with PFPA-phosphate. Carbohydrate conjugation was then achieved photochemically by irradiating the dispersion of iron oxide nanoparticles and carbohydrate followed by dialysis [112, 113].

2.5 Silica nanoparticles

SNPs are widely used in biochemistry due to their outstanding biocompatibility, water dispersability, stability and functionality [114–117]. Among different SNPs formats, mesoporous SNPs have over the last 20 years been developed to possess unique and advantageous properties such as tunable particle size, pore size and shape. These properties have enabled their use as drug delivery systems in for example anti-cancer therapy. Mesoporous SNPs were in this case loaded with multiple drugs and functionalized with active targeting ligands, including carbohydrates. The resulting SNPs were able to selectively target tumor cells, including multi-drug resistance (MDR) cells, leading to cancer cell death without damaging normal tissue [118].

SNP surfaces can be efficiently functionalized with carbohydrates by post-modification methods, generally involving initial functionalization of the SNPs, and subsequent conjugation of derivatized or underivatized carbohydrates. Several different conjugation chemistries have here been used, including CuAAC, amide coupling, nucleophilic substitution, and photocoupling. For example, Basu et al. synthesized azide-functionalized SNPs using ((azidomethyl)phenylethyl)-trimethoxysilane, and conjugated alkyne-functionalized carbohydrate derivatives in the presence of $CuSO_4$/sodium ascorbate or CuI/diisopropylethylamine, while heating to 70 °C in a microwave reactor [119]. Liu et al. utilized amide coupling to conjugate galactose (Gal) derivatives onto SNPs. The SNPs surface was first functionalized with *N*-(β-ethylenamine)-γ-propylamine triethyloxylsilane and lactobionic acid was then coupled to the amino-functionalized surface in the presence of amide coupling reagents [120]. Gary-Bobo et al. prepared mannose-functionalized mesoporous SNPs by coupling aminopropyl-functionalized SNPs to squarate ester-derivatized α-mannose [121]. For the photoinitiated carbohydrate conjugation to SNPs, a method developed in our laboratory the nanoparticles were first functionalized with PFPA-silane, after which the carbohydrates were conjugated by irradiation in the presence of carbohydrates. Using this methodology we have for example prepared carbohydrate-functionalized SNPs from different mono- and oligosaccharides [15, 76, 122–124].

3 Affinity enhancement

Carbohydrate-mediated interactions are generally weak, where for example the K_d values of carbohydrate–lectin interactions are in the range of μM-mM. This is orders of magnitude lower than enzyme-substrate or antibody-antigen interactions, where the affinities are commonly on the order of nM. To compensate for this, nature uses the so-called

multivalency- or clustering effect where multiple copies of glycan ligands are conjugated on peptides, proteins or lipids. The result of this multiple ligand presentation is significantly enhanced affinity with carbohydrate-binding proteins.

Nanomaterials are excellent multivalent scaffolds that can enable high affinities for carbohydrate-binding proteins. The affinity enhancement, however, is to a large extent affected by how the carbohydrate ligands are displayed on the nanomaterials. In this respect, we set out to study how the ligand density, the spacer linker length, and the nanoparticle size impact the binding affinity of glyconanomaterials with lectins. In order to achieve this, we developed four characterization methods to determine the K_d values of glyconanoparticles interacting with lectins. These include fluorescence competition assay [123], isothermal microcalorimetry [14], dynamic light scattering [13], and super microarrays [15]. Thus, various carbohydrate ligands were immobilized on AuNPs, and the binding affinities for specific lectins were measured. The results showed that the binding affinity of carbohydrate ligands conjugated on AuNPs were 3–5 orders of magnitude higher than those of free carbohydrate ligands.

To investigate the factors that influence the binding affinity, we conjugated carbohydrates to AuNPs having different ligand density, spacer lengths, and also varied the diameter of the AuNPs. It was found that the binding affinity displayed an optimal value depending on the spacer length and structure, in part due to the increased freedom of ligands when a longer spacer linkage was used [10]. We then prepared mannose-conjugated AuNPs with varying mannose density. Binding studies with Con A showed that, initially, the affinity increased with the ligand density, and then remained more or less constant [11, 89]. Higher ligand density might impose steric hindrance, thus reducing the lectin access to the surface-bound carbohydrate ligand. Other groups have also studied this effect, and in the work of Penadés et al., lactose was coated on AuNPs to various density and the binding affinity for *Viscum album* agglutinin (VAA) was determined. It was found that binding of AuNPs with 100% density was weaker than lower percentage densities [125]. Similar results have also been observed by others for lectins interacting with carbohydrate ligands immobilized on flat surfaces as well as nanoparticles [87, 126].

In addition, we found that nanoparticles selectively enhanced high affinity interactions. In our studies on the variants of cyanovirin-N lectins, by conjugating Man2 or Man3 on AuNPs, the affinity enhancement was 21–86 fold higher for the stronger binding domain than the weaker binding domain [12]. In another work, we prepared carbohydrate microarrays and glyconanoparticle microarrays, and treated them with fluorescently labeled lectins. The higher affinity ligands displayed stronger signals on glyconanoparticle microarrays than the carbohydrate microarrays, whereas the weaker ligands showed lower signals on glyconanoparticle microarrays than the carbohydrate microarrays [123].

4 Glyconanomaterials in imaging

4.1 Fluorescence

Fluorescence remains one of the most popular techniques for bioimaging, presenting clear images for the identification and tracking of molecular recognition events. Presently, three

major fluorescent materials are most widely used: Organic dyes, inorganic nanoparticles and fluorescent polymers. In this section, we will discuss examples where the fluorescent glyconanomaterials are used in bioimaging. The section is organized by the type of luminescent nanomaterials used to label glycans.

4.1.1 Organic dye-doped nanomaterials—Organic dyes continue to be the label of choice due to the availability of a wide variety of commercial products of diverse structures, functionalities, solubility, and spectral properties. However, organic dyes have relatively poor photostability, and when exposed to light, can photobleach, resulting in a decrease in fluorescence intensity [127]. By entrapping the fluorescent dye inside nanoparticles, the dye molecules are protected from being directly exposed to the environmental oxygen, and thus the photostability can be greatly enhanced [128, 129]. Furthermore, because a large number of dye molecules can be embedded inside a nanoparticle, high fluorescence emission can be obtained, the intensity of which exceeds the dye molecule itself or even QDs [130]. Of different nanomaterials, SNPs are highly suitable for dye doping, being easy to synthesize and chemically functionalize, and generally being more stable compared to other luminescent nanoparticles.

We employed dye-doped SNPs to study the interactions of glycans with bacteria [122]. In this case, the glycans were labeled with fluorescein isothiocyanate (FITC)-doped SNPs using the photocoupling chemistry described in the above. The developed fluorescent SNPs (FSNPs) could subsequently be used to monitor cell-glycan interactions. Thus, D-mannose-functionalized FSNPs showed selective binding to *E. coli* strain ORN 178 through interaction with the Man-binding lectin FimH on its pili (Fig. 4(a)). In comparison, no fluorescence was visible on the *E. coli* strain ORN 208 that lacks the FimH lectin (Fig. 4(b)). In another example, maltoheptaose was conjugated to various nanoparticles including FITC-doped SNPs using the same photocoupling chemistry. When the maltoheptaose-conjugated nanoparticles were treated with *E. coli*, strong interactions with the bacteria cells occurred (Figs. 5(a) and 5(b)). Particle internalization by the bacteria cells was observed when maltoheptaose-conjugated iron oxide nanoparticle were treated with *E. coli* (Fig. 5(c)) [113].

4.1.2 Quantum dots—Semiconducting nanoparticles such as QDs exhibit outstanding optical properties such as tunable emission through size control, high fluorescence intensity and broad excitation range in comparison to organic dyes. They are therefore becoming an important tool for bioimaging applications. For example, Mukhopadhyay et al. synthesized α-D-mannoside-coated CdS QDs, which were subsequently fed to *E. coli* cultures. Confocal fluorescence microscopy images showed QD-induced aggregation of *E. coli* ORN 178, while *E. coli* ORN 208 showed no aggregation [93].

Furthermore, cells can also be labeled by QDs. In a work of Robinson et al., GlcNAc-functionalized QDs were incubated with fresh sperm cells, and confocal fluorescence microscope images were taken (Fig. 6). Sea-urchin sperms exhibited higher fluorescence intensity on the head when treated with GlcNAc-QDs, whereas more uniform fluorescence was observed on mouse sperms treated with mannosylated QDs. The authors concluded that this may be the result from the different distribution of GlcNAc and Man receptors on sea-urchin and mouse sperms, respectively [131]. In another example by Coulon et al.,

galactose- and mannose-coated CdTe QDs were successfully used to label living yeast cells *Kluyveromyces bulgaricus* and *Saccharomyces cerevisiae*, respectively [132].

A major drawback of CdSe-based QDs is their high toxicity. It was reported that the outer coating of the QDs may be detached and expose the metal core when subjected to oxidation and pH change [133]. Furthermore, oxidation by reactive oxygen species (ROS) may release toxic ions such as Cd^{2+} which might cause decrease in fluorescence intensity during this process. By comparison, silicon nanoparticles, another type of fluorescent QDs, are much less toxic than cadmium-based QDs [134], and can also be applied to glycan–cell interaction. For example, Li et al. used silicon nanoparticles as luminescent probes for detecting and labeling cells. Strong fluorescence in MCF-7 breast cancer cells was thus observed upon incubation with mannose-conjugated silicon nanoparticles. Furthermore, no morphological damage could be detected on the MCF-7 cells even after 48 h incubation, whereas the tested CdTe QDs induced significant cell death in 24 h [135, 136].

4.1.3 Fluorescent polymers—Fluorescent polymers have also been used to label carbohydrates for bioimaging applications. Two classes of polymers can be used in this case: Polymers having fluorescent backbones and polymers that contain fluorescent dyes as side chain groups.

To introduce fluorescence in the backbone, fluorescent semiconducting polymers based on π–π conjugation, such as polyfluorene-, poly(phenylene ethylene)-(PPE), poly(phenylene vinylene)- and fluorene-based copolymers, were developed [137]. These structures have relatively large absorbance ranges and very high extinction coefficients (up to 30 times larger than for QDs and 200 times better than organic dyes). In addition, a shorter fluorescence lifetime allows for fast emission that can be easily detected in flow cytometry [138]. Compared to QDs, polymers also show better biocompabilities and lower toxicities, retaining their integrity and displaying higher stabilities without quenching [139, 140]. These features can be used in glyconanomaterial applications. For instance, carbohydrate-grafted PPE prepared by Bunz et al. showed strong fluorescence and tunable emission upon addition of different surfactants such as Tween 20, which induced nanoparticle dissociation [141]. In another example by Seeberger et al., mannose-grafted PPE was used to target and image *E. coli* [142].

Polymers that contain fluorescent dyes as side chain groups are generally prepared by grafting the dyes to the backbones. This was used in a study by Müller et al. who used galactose- and pyrene-grafted poly(methacrylate) copolymers to coat silica-protected MNPs. The resulting nanoparticles were successfully applied to image A549, adenocarcinomic human alveolar basal epithelial cells (Fig. 7) [143].

4.2 Magnetic resonance imaging

MRI is a powerful technique to visualize the internal structure of living organisms and is regarded a safer technique compared to X-ray computed tomography (CT) and positron emission tomography (PET), which use radioactive elements for detection. The collected MRI data, based on the spin-lattice relaxation time T_1 and spin-spin relaxation time T_2, lead

to positive or negative contrast depending on the environmental change and the material itself [144].

Using MRI *in vitro*, Huang and co-workers synthesized various magnetic glyconanoparticles (MGNPs) in order to estimate the binding affinities with different lectins [145]. Con A, possessing four Man-selective binding sites, acted as a crosslinker that induced aggregation of the Man-MGNPs. As a result, T_2 decreased with increasing Con A concentration, while T_2 of the unfunctionalized nanoparticles remained unchanged (Fig. 8(c)). Similarly, wheat germ agglutinin (WGA, a GlcNAc and Sia-selective lectin) showed aggregation with GlcNAc-MGNPs whereas no change was observed for Gal-MGNPs (Fig. 8(d)).

In vivo MRI imaging is also possible where the glyconanoparticles can be used to detect diseases. To visualize brain diseases such as inflammation, Davis and coworkers designed bloodborne leukocyte mimicking sLe^x-functionalized MNPs that could target CD62 adhesion molecules (E- and P-selectin) on activated endothelial cells. These adhesion molecules played an important role in initial recruitment of leukocytes to the inflammation site where symptom-based diagnoses could only detect later stages. The sLe^x-MNPs could selectively label the activated cerebral endothelium, offering high potential in early disease detection (Figs. 9(a), 9(b) and 9(d)) [146].

The most clinically used MRI contrast agents for brain imaging, paramagnetic gadolinium (Gd^{3+}) compounds, are based on shortening of the spin-lattice relaxation time T_1 to provide positive contrast. A drawback of gadolinium compounds is that they are rapidly cleared from the body [147]. To overcome this problem, Gd-based nanomaterials such as polymers, carbon- and inorganic nanoparticles were developed, of which Gd(III)-derivatized AuNPs showed especially high potential for clinical uses [148–150]. This was for example shown by Penadés and coworkers, who prepared hybrid AuNPs coated with thiol-functionalized carbohydrates and Gd(III)-coordinated tetraazacyclododecane triacetic acid (DO3A), and subsequently applied them in MRI imaging [151].

4.3 PET/single-photo emission computed tomography (SPECT)/CT

PET, SPECT and CT are widely used techniques in medical imaging [152, 153]. SPECT and PET provide 3D images by detecting the gamma rays from gamma-emitting radionuclides and positron-emitting radio-nuclides, respectively. The combination of CT with PET or SPECT could also help locate abnormal tissue more precisely [154]. Recently, glyconanomaterials were utilized in PET/CT and SPECT/CT systems. For example, Yang and coworkers prepared ^{111}In-labeled polymer micelles functionalized with glucosamine (GlcN) as tumor tracers. Higher radioactivity was in this case found in the tumor, liver and spleen [155, 156]. Although the results did not show active targeting clearly, the study still provided valuable data for further glyconanomaterial design. In another investigation, Davis et al. loaded GlcNAc-coated SWCNTs with a radiotracer ($Na^{125}I$). The functionalized SWCNTs could specifically target the lung, whereas the free radiotracer resulted in low selectivity [55]. Furthermore, the SPECT/CT signals from the loaded SWCNTs remained strong even after 24 h incubation. In contrast, a clear signal decrease was observed for free radiotracers due to the fast clearance from the body.

5 Glyconanomaterials in diagnosis and therapeutics

5.1 Glyconanomaterial-cell interactions *in vitro*

Glyconanomaterials are frequently used to induce cellular interactions or aggregation through lectin receptors on the cell surfaces. This was for example demonstrated by Sun and coworkers, in studies where galactose-derivatized SWCNTs were used to induce the aggregation of *E. coli* O157:H7, while mannose-functionalized SWCNTs led to the agglutination of *B. subtilis* spores [157, 158]. In another example, Bertozzi and co-workers treated Chinese hamster ovary (CHO) cells with CNTs conjugated with a mucin mimic (α-GalNAc-lipid/β-GalNAc-lipid) in the presence of HPA. Strong specific binding was observed between the α-GalNAc-lipid and HPA, inducing cell crosslinking, while only physical absorption could be found for β-GalNAc-lipid from fluorescence microscopy [38].

Glyconanomaterials can furthermore undergo cell internalization. For example, Yang et al. used lactose-and galactose-functionalized CdSeS/ZnS QDs to study their uptake by HepG2 liver carcinoma cells. Optical-and fluorescence imaging indicated cellular uptake of the QDs, presumably through an endocytosis mechanism (Fig. 10) [159]. Similarly, QDs coated with galactose-grafted poly(benzaldehyde-polyethylene glycol)-poly(DL-lactide) indicated internalization in HepG2 cells in a study by Cai et al. [160]. Other cell lines have also been studied, where for example Ao-yama et al. prepared CdSe QDs coated with cellobiose, lactose, maltose and maltoheptaose, and studied their cellular uptake by HeLa cells. The results showed that the endocytosis was highly size-dependent. The optimal size for cellular uptake was around 50 nm, whereas very low amounts of larger (>100 nm) or smaller (<15 nm) QDs were found in the cells [161].

Glycan-mediated interactions of glyconanomaterial with bacteria has been studied in our laboratory. A range of different carbohydrates were conjugated on a variety of nanoparticles. We found that while Man-NPs bound to the pili of bacteria cells via the Man-binding receptor Fim H (Fig. 4(a)), conjugation of maltoheptaose to nanoparticles induced strong interactions with *E. coli* (Figs. 5(a) and 5(b)). Maltoheptaose-conjugated iron oxide nanoparticles were internalized by *E. coli*, where the nanoparticle uptake was confirmed by TEM thin section samples (Fig.5(c)) [113]. When cyclodextrin-conjugated nanoparticles were instead used, no surface binding or cellular uptake was observed. These results demonstrate that the nature of the carbohydrate ligand dictates how the nanoparticles interact with bacterial cells. The results also pave the way for tailor-making glyconanomaterials to target specific cells for imaging and therapeutic applications.

Glyconanoparticles can also be used to differentiate cell types. In a study by El-Boubbou et al., different cell lines were incubated with an array of carbohydrate-functionalized iron oxide MNPs (Fig. 11) [145]. MRI and Prussian blue-staining assay were utilized to quantify the uptake of the glyco-MNPs, showing different patterns of binding and uptake resulting from the distinct lectin receptors on the cells. Using the statistical method of linear discriminant analysis, the authors were able to distinguish normal cells from cancer cells, and also the specific type of cancer cells.

5.2 Glyconanomaterial-cell interaction *in vivo*

In a study by Kikkeri et al., different carbohydrate-capped QDs were prepared to evaluate the distribution of glyconanoparticles *in vivo* [98]. QDs modified with PEG, Man-PEG and D-galactosamine (GalN)-PEG were dispersed in PBS and injected into mice via the tail vein. It was found that clusters of Man-QDs and GalN-QDs were visible in the liver, while mice treated with PBS and PEG-QDs showed very little fluorescence (Fig. 12). The authors concluded that mannose receptors on Kupffer cells and sinusoidal endothelial cells played a crucial role in QD-Man binding, while the asialoglycoprotein receptor (ASGP-R) on hepatocytes interacted with the GalN-QDs. Interestingly, cell viability studies showed that QDs coated with carbohydrates were considerably less toxic than those with PEG coating.

Another investigation was conducted by Ohyanagi et al. to study the distribution of glyco-QDs *in vivo* [162]. Near IR fluorescence images of mice injected with carbohydrate-coated QDs exhibited significant differences in time-dependent distribution (Fig. 13). QDs derivatized with sialyl *N*-acetyllactosamine (sialyl-LacNAc) accumulated in the spleen and intestine rapidly, while LacNAc-functionalized QDs and Le^x-QDs were localized in the liver, and no preferential distribution was observed for sLe^x-QDs. However, the fluorescence decreased significantly after 2 h, indicating the poor stability of this type of QDs *in vivo*.

5.3 Therapy

The potential for therapeutic applications of glycon-anomaterials have furthermore been demonstrated. A relatively early example involved the use of glyconanoparticles in anti-adhesion therapy. In this case, Rojo et al. synthesized lactose-AuNPs and glucose-AuNPs, and mixed them with B16F10 melanoma cells at 37 °C for 5 min, followed by injection into C57/B16 mice to test the inhibition of lung metastasis. The authors found that the lung of mice treated with lactose-AuNPs had fewer foci, while a high number was observed for the mice treated with glucose-AuNPs (Fig. 14). This result suggested that lactose may play an important role in melanoma cell metastasis, and that lactose-AuNPs were effective in preventing tumor cell adhesion [84].

Anti-viral therapy represents another area where glyconanomaterials can be used. For example, it has been established that the HIV envelope glycoprotein gp120 contains clusters of high mannose glycans that are recognized by human monoclonal antibody 2G12. This glycan presentation was mimicked in a study by Penadés and coworkers, where AuNPs covered by a monolayer of oligomannosides were synthesized to compete with gp120 for cell binding. SPR results confirmed the strong affinity of these glyconanoparticles to 2G12. In addition, after treating 2G12 with glycon-anoparticles, gp120 was not able to bind 2G12 [19, 163]. The authors further showed that pre-treatment with oligomannoside-coated AuNPs could reduce and perhaps inhibit the infection of Raji dendritic cell-specific intercellular adhesion molecule-3-grabbing non-integrin (DC-SIGN)-transfected lymphoblastoid B cells by HIV-1 recombinant viruses JR-Renilla (R5) or NL4.3-Renilla (X4). A 50% mannose density on the AuNPs was sufficient to reach significant inhibition, and the best AuNPs were found to present 56 linear tetra-mannosides (Manα1-2Manα1-2Manα1-3Manα1-R) [164].

Based on the fact that Ebola virus infections are mediated by the interaction between the C-type lectin DC-SIGN on cell surfaces with the mannose-containing glycans on the viral particle, it was hypothesized that mannose-functionalized nanoparticles could inhibit the infection. This was addressed by Luczkowiak et al., who conducted a study where fullerenes were functionalized with mono- and branched mannosides and galactosides. The IC_{50}-values were in this case estimated to 0.3 μM with branched mannose-fullerenes connected to flexible chains [165]. Further improvement in inhibition efficiency could be achieved by specific carbohydrate selection, ligand density, and chain flexibility.

Photodynamic therapy (PDT) uses light- activated photosensitizers to generate reactive oxygen species and thus destroying cells and tissues. An advantage of PDT treatment is that it can be specifically focused on the disease site without affecting other parts of the body. The drawback, on the other hand, is the penetration depth of light that may not reach the disease sites [166]. A few reports have evaluated the use of glyconanomaterials in PDT [167, 168]. For example, Brevet et al. embedded photosensitizers inside mannose-coated mesoporous SNPs, and applied them to human breast cancer cells. The results showed 99% cell death under light irradiation, in comparison to 19% without irradiation [167].

Ferromagnetic and ferroelectric MNPs exhibit hyperthermia properties, i.e., the increase in temperature induced by an external alternating magnetic field [169-171]. This technique has been used in cancer therapy since the 1970s, whereby the temperature increase causes cell damage and destruction of tumor cells [172-176] Preliminary studies demonstrating the potential of glyco-MNPs in hyperthermia therapy was recently reported [110]. MNPs coated with rhamnose, mannose and ribose were prepared, and the specific absorption rate (SAR) data was used to measure the hyperthermal efficiency. The results indicated that remarkable heat could be generated by the MNPs, where for example the SAR of 16 nm rhamnose-MNPs could reach a maximum of 185 W/g.

6 Conclusions and perspectives

Nanoscience and nanotechnology have witnessed rapid development over especially the last three decades. Nanomaterials of various chemical composition, structure, morphology, size, shape, and surface functionality are now being synthesized, and new nanomaterials having unique chemical, physical and biological properties are appearing in literature on a daily basis. The study of glyconanomaterials, on the other hand, is a new field and the progress has been relatively lagging. This has primarily been due to challenges in the glycosciences area, partially owing to the complexity and difficulty in chemically synthesizing and derivatizing glycan structures. The vast majority of glyconanomaterials are thus made from simple and inexpensive carbohydrate structures such as monosaccharides. Nonetheless, the conjugation chemistries are mostly general and can be applied to attach these carbohydrates to a wide variety of nanomaterials.

One important feature of glyconanomaterials is their multivalency. The nanomaterial acts as a multi-valent scaffold carrying multiple copies of carbohydrate molecules, thus amplifying the binding affinity with the recognition receptors. Glyconanomaterials can in this context be considered as simple glycan-presenting cell/virus-mimics able to interact with other

biological entities. Compared to free, un-bound carbohydrates, glyconanomaterials exhibit several orders of magnitude higher binding affinity with lectins. This multivalency effect, however, is highly dependent on how the carbohydrate ligands are displayed on the nanomaterial surface. The conjugation chemistry, spacer linkage, ligand density and spatial arrangement govern the binding affinity and influence the interactions of the glyconanomaterials with other biological entities. A comprehensive understanding of these issues will no doubt be important not only to the field in general but also in the rational design of effective glyconano-materials for biomedical applications.

The applications of glyconanomaterials take advantage of the recognition ability of the carbohydrate ligands, and the unique physical properties of the nanomaterials. The carbohydrate ligand selectively interacts with the receptors on cell surface, and trigger binding, cell agglomeration, or particle internalization. When the nanomaterials possess unique physical properties, the molecular events can be effectively translated into visible or readable signals allowing for imaging and detection of disease states. Thus, glyconanomaterials have been used in fluorescence, MRI and PET/CT imaging to distinguish different cell lines or locate tumors *in vitro* and *in vivo*. Applications of glyconanomaterials as therapeutics have also started to emerge, for example, for photodynamic and hyperthermia therapy.

With the further development of glyconanomaterials, more and more applications will emerge. For biomedical uses, several important challenges need to be addressed. For example, these nanomaterials should show good biocompatibility and no/minimal toxicity to avoid exerting damage to tissues and to reduce inflammation. For increased control in drug delivery, controlled release mechanisms need to be deviced, and the residence time increased to maximize the efficiency. Selective targeting is also of importance, reducing the therapeutic dose without harming normal tissues. More recently, the combination of different nanomaterials with multiple functions is gaining interest. Multiple MNPs and QDs can for example be encapsulated in SNPs, resulting in nanoparticles with both luminescent and magnetic properties. Such hybrid nanomaterials have the potential to enhance the versatilities and efficiencies of the systems. We believe that these developments, together with others, will enable a successful range of new applications for glyconanomaterials.

Acknowledgments

The authors are grateful for financial supports from the National Institutes of Health (Nos. R01GM080295 and 2R15GM066279), the National Science Foundation (No. CHE-1112436), the University of Massachusetts Lowell, and KTH—Royal Institute of Technology, Sweden.

References

1. Brandley BK, Schnaar RL. Cell-surface carbohydrates in cell recognition and response. J Leukocyte Biol. 1986; 40:97–111. [PubMed: 3011937]
2. Sharon N. Lectin–carbohydrate complexes of plants and animals: An atomic view. Trends Biochem Sci. 1993; 18:221–226. [PubMed: 8346557]
3. Bucior I, Burger MM. Carbohydrate–carbohydrate interactions in cell recognition. Curr Opin Struct Biol. 2004; 14:631–637. [PubMed: 15465325]

4. Lasky L. Selectins: Interpreters of cell-specific carbohydrate information during inflammation. Science. 1992; 258:964–969. [PubMed: 1439808]
5. Smith AE, Helenius A. How viruses enter animal cells. Science. 2004; 304:237–242. [PubMed: 15073366]
6. Kwong PD, Wyatt R, Robinson J, Sweet RW, Sodroski J, Hendrickson WA. Structure of an HIV gp120 envelope glycoprotein in complex with the CD4 receptor and a neutralizing human antibody. Nature. 1998; 393:648–659. [PubMed: 9641677]
7. Glabe CG, Grabel LB, Vacquier VD, Rosen SD. Carbohydrate specificity of sea urchin sperm bindin: A cell surface lectin mediating sperm–egg adhesion. J Cell Biol. 1982; 94:123–128. [PubMed: 7119010]
8. Takada A, Ohmori K, Yoneda T, Tsuyuoka K, Hasegawa A, Kiso M, Kannagi R. Contribution of carbohydrate antigens sialyl lewis A and sialyl lewis X to adhesion of human cancer cells to vascular endothelium. Cancer Res. 1993; 53:354–361. [PubMed: 7678075]
9. Kannagi R. Carbohydrate-mediated cell adhesion involved in hematogenous metastasis of cancer. Glycoconjugate J. 1997; 14:577–584.
10. Wang X, Ramström O, Yan M. Quantitative analysis of multivalent ligand presentation on gold glyconanoparticles and the impact on lectin binding. Anal Chem. 2010; 82:9082–9089. [PubMed: 20942402]
11. Wang X, Ramström O, Yan M. Glyconanomaterials: Synthesis, characterization, and ligand presentation. Adv Mater. 2010; 22:1946–1953. [PubMed: 20301131]
12. Wang X, Matei E, Deng LQ, Ramström O, Gronenborn AM, Yan M. Multivalent glyconanoparticles with enhanced affinity to the anti-viral lectin Cyanovirin-N. Chem Commun. 2011; 47:8620–8622.
13. Wang X, Ramström O, Yan M. Dynamic light scattering as an efficient tool to study glyconanoparticle–lectin interactions. Analyst. 2011; 136:4174–4178. [PubMed: 21858301]
14. Wang X, Matei E, Gronenborn AM, Ramström O, Yan M. Direct measurement of glyconanoparticles and lectin interactions by isothermal titration calorimetry. Anal Chem. 2012; 84:4248–4252. [PubMed: 22548468]
15. Wang X, Matei E, Deng LQ, Koharudin L, Gronenborn AM, Ramström O, Yan M. Sensing lectin–glycan interactions using lectin super-microarrays and glycans labeled with dye-doped silica nanoparticles. Biosens Bioelectron. 2013; 47:258–264. [PubMed: 23584388]
16. Jayaraman N. Multivalent ligand presentation as a central concept to study intricate carbohydrate–protein interactions. Chem Soc Rev. 2009; 38:3463–3483. [PubMed: 20449063]
17. Mahon E, Aastrup T, Barboiu M. Multivalent recognition of lectins by glyconanoparticle systems. Chem Commun. 2010; 46:5491–5493.
18. Liang CH, Wang CC, Lin YC, Chen CH, Wong CH, Wu CY. Iron oxide/gold core/shell nanoparticles for ultrasensitive detection of carbohydrate–protein interactions. Anal Chem. 2009; 81:7750–7756. [PubMed: 19689135]
19. Marradi M, Di Gianvincenzo P, Enríquez-Navas PM, Martínez-Ávila OM, Chiodo F, Yuste E, Angulo J, Penadés S. Gold nanoparticles coated with oligomannosides of HIV-1 glycoprotein gp120 mimic the carbohydrate epitope of antibody 2G12. J Mol Biol. 2011; 410:798–810. [PubMed: 21440555]
20. Varma AJ, Kennedy JF, Galgali P. Synthetic polymers functionalized by carbohydrates: A review. Carbohydr Polym. 2004; 56:429–445.
21. Voit B, Appelhans D. Glycopolymers of various architectures—more than mimicking nature. Macromol Chem Phys. 2010; 211:727–735.
22. Sunasee R, Narain R. Glycopolymers and glyconanoparticles in biomolecular recognition processes and vaccine development. Macromol Biosci. 2013; 13:9–27. [PubMed: 23042762]
23. Ahmed M, Wattanaarsakit P, Narain R. Recent advances in the preparation of glycopolymer bioconjugates. Eur Polym J. 2013; 49:3010–3033.
24. Yilmaz G, Becer CR. Precision glycopolymers and their interactions with lectins. Eur Polym J. 2013; 49:3046–3051.
25. Chabre YM, Roy R. Recent trends in glycodendrimer syntheses and applications. Curr Top Med Chem. 2008; 8:1237–1285. [PubMed: 18855708]

26. Shiao TC, Roy R. Glycodendrimers as functional antigens and antitumor vaccines. New J Chem. 2012; 36:324–339.
27. Hatano K, Matsuoka K, Terunuma D. Carbosilane glycodendrimers. Chem Soc Rev. 2013; 42:4574–4598. [PubMed: 23257960]
28. Khan SA, Adak A, Vasudeva Murthy R, Kikkeri R. Recent advances in the metallo-glycodendrimers and its potential applications. Inorg Chim Acta. 2014; 409:26–33.
29. Kitamoto D, Morita T, Fukuoka T, Konishi MA, Imura T. Self-assembling properties of glycolipid biosurfactants and their potential applications. Curr Opin Colloid Interface Sci. 2009; 14:315–328.
30. Hashim R, Sugimura A, Minamikawa H, Heidelberg T. Nature-like synthetic alkyl branched-chain glycolipids: A review on chemical structure and self-assembly properties. Liq Cryst. 2011; 39:1–17.
31. Jayaraman N, Maiti K, Naresh K. Multivalent glycoliposomes and micelles to study carbohydrate–protein and carbohydrate–carbohydrate interactions. Chem Soc Rev. 2013; 42:4640–4656. [PubMed: 23487184]
32. Lemarchand C, Gref R, Couvreur P. Polysaccharidedecorated nanoparticles. Eur J Pharm Biopharm. 2004; 58:327–341. [PubMed: 15296959]
33. Dias AMGC, Hussain A, Marcos AS, Roque ACA. A biotechnological perspective on the application of iron oxide magnetic colloids modified with polysaccharides. Biotechnol Adv. 2011; 29:142–155. [PubMed: 20959138]
34. Daniel-da-Silva, AL.; Trindade, T. Biofunctional composites of polysaccharides containing inorganic nanoparticles. In: Abbass, H., editor. Advances in Nanocomposite Technology. InTech; Rijeka: 2011. p. 275-298.
35. Covaliu C, Berger D, Matei C, Diamandescu L, Vasile E, Cristea C, Ionita V, Iovu H. Magnetic nanoparticles coated with polysaccharide polymers for potential biomedical applications. J Nanopart Res. 2011; 13:6169–6180.
36. Lam CW, James JT, McCluskey R, Arepalli S, Hunter RL. A review of carbon nanotube toxicity and assessment of potential occupational and environmental health risks. Crit Rev Toxicol. 2006; 36:189–217. [PubMed: 16686422]
37. Chen X, Lee GS, Zettl A, Bertozzi CR. Biomimetic engineering of carbon nanotubes by using cell surface mucin mimics. Angew Chem Int Ed. 2004; 43:6111–6116.
38. Chen X, Tam UC, Czlapinski JL, Lee GS, Rabuka D, Zettl A, Bertozzi CR. Interfacing carbon nanotubes with living cells. J Am Chem Soc. 2006; 128:6292–6293. [PubMed: 16683774]
39. Khiar N, Leal MP, Baati R, Ruhlmann C, Mioskowski C, Schultz P, Fernandez I. Tailoring carbon nanotube surfaces with glyconanorings: New bionanomaterials with specific lectin affinity. Chem Commun. 2009:4121–4123.
40. Feng W, Luo RM, Xiao J, Ji PJ, Zheng ZG. Self-assembly of sugar-based amphiphile on carbon nanotubes for protein adsorption. Chem Eng Sci. 2011; 66:4807–4813.
41. Murthy BN, Zeile S, Nambiar M, Nussio MR, Gibson CT, Shapter JG, Jayaraman N, Voelcker NH. Self assembly of bivalent glycolipids on single walled carbon nanotubes and their specific molecular recognition properties. RSC Adv. 2012; 2:1329–1333.
42. Wu P, Chen X, Hu N, Tam UC, Blixt O, Zettl A, Bertozzi CR. Biocompatible carbon nanotubes generated by functionalization with glycodendrimers. Angew Chem Int Ed. 2008; 47:5022–5025.
43. Sudibya HG, Ma JM, Dong XC, Ng S, Li LJ, Liu XW, Chen P. Interfacing glycosylated carbon-nanotube-network devices with living cells to detect dynamic secretion of biomolecules. Angew Chem Int Ed. 2009; 48:2723–2726.
44. Chen QS, Wei WL, Lin JM. Homogeneous detection of concanavalin A using pyrene-conjugated maltose assembled graphene based on fluorescence resonance energy transfer. Biosens Bioelectron. 2011; 26:4497–4502. [PubMed: 21621405]
45. Chen YN, Vedala H, Kotchey GP, Audfray A, Cecioni S, Imberty A, Vidal S, Star A. Electronic detection of lectins using carbohydrate-functionalized nanostructures: Graphene versus carbon nanotubes. ACS Nano. 2011; 6:760–770. [PubMed: 22136380]
46. Kuzmany H, Kukovecz A, Simon F, Holzweber M, Kramberger C, Pichler T. Functionalization of carbon nanotubes. Synth Met. 2004; 141:113–122.

47. Georgakilas V, Otyepka M, Bourlinos AB, Chandra V, Kim ND, Kemp KC, Hobza P, Zboril R, Kim KS. Functionalization of graphene: Covalent and non-covalent approaches, derivatives and applications. Chem Rev. 2012; 112:6156–6214. [PubMed: 23009634]
48. Park J, Yan M. Covalent functionalization of graphene with reactive intermediates. Acc Chem Res. 2012; 46:181–189. [PubMed: 23116448]
49. Prato M. [60]Fullerene chemistry for materials science applications. J Mater Chem. 1997; 7:1097–1109.
50. Wudl F. Fullerene materials. J Mater Chem. 2002; 12:1959–1963.
51. Gorityala BK, Ma JM, Wang X, Chen P, Liu XW. Carbohydrate functionalized carbon nanotubes and their applications. Chem Soc Rev. 2010; 39:2925–2934. [PubMed: 20585681]
52. Chen YN, Star A, Vidal S. Sweet carbon nanostructures: Carbohydrate conjugates with carbon nanotubes and graphene and their applications. Chem Soc Rev. 2013; 42:4532–4542. [PubMed: 23247183]
53. Pinson J, Podvorica F. Attachment of organic layers to conductive or semiconductive surfaces by reduction of diazonium salts. Chem Soc Rev. 2005; 34:429–439. [PubMed: 15852155]
54. Ragoussi ME, Casado S, Ribeiro-Viana R, de la Torre G, Rojo J, Torres T. Selective carbohydrate–lectin interactions in covalent graphene- and SWCNT-based molecular recognition systems. Chem Sci. 2013; 4:4035–4041.
55. Hong SY, Tobias G, Al-Jamal KT, Ballesteros B, Ali-Boucetta H, Lozano-Perez S, Nellist PD, Sim RB, Finucane C, Mather SJ, et al. Filled and glycosylated carbon nanotubes for *in vivo* radioemitter localization and imaging. Nat Mater. 2010; 9:485–490. [PubMed: 20473287]
56. Prato M, Li QC, Wudl F, Lucchini V. Addition of azides to fullerene C_{60}: Synthesis of azafulleroids. J Am Chem Soc. 1993; 115:1148–1150.
57. Holzinger M, Abraham J, Whelan P, Graupner R, Ley L, Hennrich F, Kappes M, Hirsch A. Functionalization of single-walled carbon nanotubes with (R-) oxycarbonyl nitrenes. J Am Chem Soc. 2003; 125:8566–8580. [PubMed: 12848565]
58. Leinonen H, Pettersson M, Lajunen M. Water-soluble carbon nanotubes through sugar azide functionalization. Carbon. 2011; 49:1299–1304.
59. Liu LH, Yan M. Simple method for the covalent immobilization of graphene. Nano Lett. 2009; 9:3375–3378. [PubMed: 19670850]
60. Liu LH, Zorn G, Castner DG, Solanki R, Lerner MM, Yan M. A simple and scalable route to wafer-size patterned graphene. J Mater Chem. 2010; 20:5041–5046. [PubMed: 24155570]
61. Liu LH, Yan M. Functionalization of pristine graphene with perfluorophenyl azides. J Mater Chem. 2011; 21:3273–3276.
62. Liu LH, Nandamuri G, Solanki R, Yan M. Electrical properties of covalently immobilized single-layer graphene devices. J Nanosci Nanotechnol. 2011; 11:1288–1292. [PubMed: 21456173]
63. Zorn G, Liu LH, Árnadóttir L, Wang H, Gamble LJ, Castner DG, Yan M. X-ray photoelectron spectroscopy investigation of the nitrogen species in photoactive perfluorophenylazide-modified surfaces. J Phys Chem C. 2014; 118:376–383.
64. Michalak J, Zhai HB, Platz MS. The photochemistry of various para-substituted tetrafluorophenyl azides in acidic media and the formation of nitrenium ions. J Phys Chem. 1996; 100:14028–14036.
65. Gritsan, NP.; Platz, MS. Kinetics and spectroscopy of substituted phenylnitrenes. In: Richard, J.; Tidwell, T., editors. Advances in Physical Organic Chemistry. Academic Press; Waltham: 2001. p. 255-304.
66. Liu LH, Yan M. Perfluorophenyl azides: New applications in surface functionalization and nanomaterial synthesis. Acc Chem Res. 2010; 43:1434–1443. [PubMed: 20690606]
67. Vyas, S.; Winter, AH.; Hadad, CM. Theory and computation in the the study of nitrenes and their excited-state photoprecursors. In: Falvey, D.; Gudmundsdottir, A., editors. Nitrenes and Nitrenium Ions. Wiley & Sons; Hoboken: 2013. p. 33-76.
68. Yan M, Cai SX, Keana JFW. Photochemical and thermal reactions of C_{60} with N-succinimidyl 4-azido-2,3,5,6-tetrafluorobenzoate: A new method for functionalization of C_{60}. J Org Chem. 1994; 59:5951–5954.

69. Pastine SJ, Okawa D, Kessler B, Rolandi M, Llorente M, Zettl A, Fréchet JMJ. A facile and patternable method for the surface modification of carbon nanotube forests using perfluoroarylazides. J Am Chem Soc. 2008; 130:4238–4239. [PubMed: 18331043]
70. Kong N, Shimpi M, Ramström O, Yan M. Functionalization of carbohydrate-presenting single-walled carbon nanotubes using microwave-assisted phenylnitrene addition and their biorecognition applications. Abstr Pap Am Chem Soc. 2013; 245
71. Kelly KL, Coronado E, Zhao LL, Schatz GC. The optical properties of metal nanoparticles: The influence of size, shape, and dielectric environment. J Phys Chem B. 2002; 107:668–677.
72. Aslan K, Zhang J, Lakowicz JR, Geddes CD. Saccharide sensing using gold and silver nanoparticles—a review. J Fluoresc. 2004; 14:391–400. [PubMed: 15617381]
73. Wang ZX, Ma LN. Gold nanoparticle probes. Coord Chem Rev. 2009; 253:1607–1618.
74. Marradi, M.; Martín-Lomas, M.; Penadés, S. Glyconan-oparticles: Polyvalent tools to study carbohydrate-based interactions. In: Derek, H., editor. Advances in Carbohydrate Chemistry and Biochemistry. Elsevier; Amsterdam: 2010. p. 211-290.
75. Saha K, Agasti SS, Kim C, Li X, Rotello VM. Gold nanoparticles in chemical and biological sensing. Chem Rev. 2012; 112:2739–2779. [PubMed: 22295941]
76. Jayawardena HSN, Wang X, Yan M. Classification of lectins by pattern recognition using glyconanoparticles. Anal Chem. 2013; 85:10277–10281. [PubMed: 24079754]
77. Craig D, Simpson J, Faulds K, Graham D. Formation of SERS active nanoparticle assemblies via specific carbohydrate–protein interactions. Chem Commun. 2013; 49:30–32.
78. Kong XM, Yu Q, Lv ZP, Du XZ. Tandem assays of protein and glucose with functionalized core/shell particles based on magnetic separation and surface-enhanced Raman scattering. Small. 2013; 9:3259–3264. [PubMed: 23585333]
79. de Souza AC, Halkes KM, Meeldijk JD, Verkleij AJ, Vliegenthart JFG, Kamerling JP. Synthesis of gold glyconanoparticles: Possible probes for the exploration of carbohydrate-mediated self-recognition of marine sponge cells. Eur J Org Chem. 2004; 2004:4323–4339.
80. de la Fuente JM, Barrientos AG, Rojas TC, Rojo J, Cañada J, Fernández A, Penadés S. Gold glyconanoparticles as water-soluble polyvalent models to study carbohydrate Interactions. Angew Chem Int Ed. 2001; 40:2257–2261.
81. Kulkarni AA, Fuller C, Korman H, Weiss AA, Iyer SS. Glycan encapsulated gold nanoparticles selectively inhibit shiga toxins 1 and 2. Bioconjugate Chem. 2010; 21:1486–1493.
82. Reynolds AJ, Haines AH, Russell DA. Gold glyconanoparticles for mimics and measurement of metal ion-mediated carbohydrate-carbohydrate interactions. Langmuir. 2006; 22:1156–1163. [PubMed: 16430279]
83. Nolting B, Yu JJ, Liu GY, Cho SJ, Kauzlarich S, Gervay-Hague J. Synthesis of gold glyconanoparticles and biological evaluation of recombinant gp120 interactions. Langmuir. 2003; 19:6465–6473.
84. Rojo J, Díaz V, de la Fuente JM, Segura I, Barrientos AG, Riese HH, Bernad A, Penadés S. Gold glyconanoparticles as new tools in antiadhesive therapy. ChemBioChem. 2004; 5:291–297. [PubMed: 14997521]
85. de Paz JL, Ojeda R, Barrientos ÁG, Penadés S, Martín-Lomas M. Synthesis of a Ley neoglycoconjugate and Le^y-functionalized gold glyconanoparticles. Tetrahedron: Asymmetry. 2005; 16:149–158.
86. de la Fuente JM, Eaton P, Barrientos AG, Menéndez M, Penadés S. Thermodynamic evidence for Ca^{2+}-mediated self-aggregation of lewis X gold glyconanoparticles. A model for cell adhesion via carbohydrate-carbohydrate interaction. J Am Chem Soc. 2005; 127:6192–6197. [PubMed: 15853323]
87. Schofield CL, Mukhopadhyay B, Hardy SM, McDonnell MB, Field RA, Russell DA. Colorimetric detection of *Ricinus communis* Agglutinin 120 using optimally presented carbohydrate-stabilised gold nanoparticles. Analyst. 2008; 133:626–634. [PubMed: 18427684]
88. Otsuka H, Akiyama Y, Nagasaki Y, Kataoka K. Quantitative and reversible lectin-induced association of gold nanoparticles modified with α-lactosyl-ω-mercapto-poly(ethylene glycol). J Am Chem Soc. 2001; 123:8226–8230. [PubMed: 11516273]

89. Wang X, Ramström O, Yan M. A photochemically initiated chemistry for coupling underivatized carbohydrates to gold nanoparticles. J Mater Chem. 2009; 19:8944–8949. [PubMed: 20856694]

90. Alivisatos P. The use of nanocrystals in biological detection. Nat Biotechnol. 2004; 22:47–52. [PubMed: 14704706]

91. Michalet X, Pinaud FF, Bentolila LA, Tsay JM, Doose S, Li JJ, Sundaresan G, Wu AM, Gambhir SS, Weiss S. Quantum dots for live cells *in vivo* imaging, and diagnostics. Science. 2005; 307:538–544. [PubMed: 15681376]

92. de la Fuente JM, Penadés S. Glyco-quantum dots: A new luminescent system with multivalent carbohydrate display. Tetrahedron: Asymmetry. 2005; 16:387–391.

93. Mukhopadhyay B, Martins MB, Karamanska R, Russell DA, Field RA. Bacterial detection using carbohydrate-functionalised CdS quantum dots: A model study exploiting *E coli* recognition of mannosides. Tetrahedron Lett. 2009; 50:886–889.

94. Babu P, Sinha S, Surolia A. Sugar-quantum dot conjugates for a selective and sensitive detection of lectins. Bioconjugate Chem. 2007; 18:146–151.

95. Kikkeri R, Laurino P, Odedra A, Seeberger PH. Synthesis of carbohydrate-functionalized quantum dots in microreactors. Angew Chem Int Ed. 2010; 49:2054–2057.

96. Laurino P, Kikkeri R, Seeberger PH. Continuous-flow reactor-based synthesis of carbohydrate and dihydrolipoic acid-capped quantum dots. Nat Protoc. 2011; 6:1209–1220. [PubMed: 21799489]

97. Dai Z, Kawde AN, Xiang Y, La Belle JT, Gerlach J, Bhavanandan VP, Joshi L, Wang J. Nanoparticlebased sensing of glycan-lectin interactions. J Am Chem Soc. 2006; 128:10018–10019. [PubMed: 16881623]

98. Kikkeri R, Lepenies B, Adibekian A, Laurino P, Seeberger PH. *In vitro* imaging and *in vivo* liver targeting with carbohydrate capped quantum dots. J Am Chem Soc. 2009; 131:2110–2112. [PubMed: 19199612]

99. Basiruddin SK, Ranjan Maity A, Jana NR. Glucose/galactose/dextran-functionalized quantum dots, iron oxide and doped semiconductor nanoparticles with <100 nm hydrodynamic diameter. RSC Adv. 2012; 2:11915–11921.

100. Pankhurst QA, Connolly J, Jones SK, Dobson J. Applications of magnetic nanoparticles in biomedicine. J Phys D: Appl Phys. 2003; 36:R167.

101. Laurent S, Forge D, Port M, Roch A, Robic C, Vander Elst L, Muller RN. Magnetic iron oxide nanoparticles: Synthesis, stabilization, vectorization, physicochemical characterizations, and biological applications. Chem Rev. 2008; 108:2064–2110. [PubMed: 18543879]

102. Sun C, Lee JSH, Zhang MQ. Magnetic nanoparticles in MR imaging and drug delivery. Adv Drug Delivery Rev. 2008; 60:1252–1265.

103. Gao JH, Gu HW, Xu B. Multifunctional magnetic nanoparticles: Design, synthesis, and biomedical applications. Acc Chem Res. 2009; 42:1097–1107. [PubMed: 19476332]

104. Veiseh O, Gunn JW, Zhang MQ. Design and fabrication of magnetic nanoparticles for targeted drug delivery and imaging. Adv Drug Delivery Rev. 2010; 62:284–304.

105. Cameron DG, Bensley EH, Wood P, Grayston V. Treatment of iron deficiency anaemia with saccharated iron oxide given by the intravenous route. Can Med Assoc J. 1951; 64:27–30. [PubMed: 14792458]

106. Lu M, Suh KR, Lee HZ, Cohen M, Rieves D, Pazdur R. FDA review of ferumoxytol (feraheme) for the treatment of iron deficiency anemia in adults with chronic kidney disease. Am J Hematol. 2010; 85:315–319. [PubMed: 20201089]

107. Horák D, Babič M, Jendelová P, Herynek V, Trchová M, Pientka Z, Pollert E, Hájek M, Syková E. D-Mannose-modified iron oxide nanoparticles for stem cell labeling. Bioconjugate Chem. 2007; 18:635–644.

108. Kekkonen V, Lafreniere N, Ebara M, Saito A, Sawa Y, Narain R. Synthesis and characterization of biocompatible magnetic glyconanoparticles. J Magn Magn Mater. 2009; 321:1393–1396.

109. Baccile N, Noiville R, Stievano L, Bogaert IV. Sophorolipids-functionalized iron oxide nanoparticles. Phys Chem Chem Phys. 2013; 15:1606–1620. [PubMed: 23247504]

110. Lartigue L, Innocenti C, Kalaivani T, Awwad A, Sanchez Duque MDM, Guari Y, Larionova J, Guérin C, Montero JLG, Barragan-Montero V, et al. Water-dispersible sugar-coated iron oxide

nanoparticles. An evaluation of their relaxometric and magnetic hyperthermia properties. J Am Chem Soc. 2011; 133:10459–10472. [PubMed: 21604803]

111. Kouyoumdjian H, Zhu DC, El-Dakdouki MH, Lorenz K, Chen JJ, Li W, Huang XF. Glyconanoparticle aided detection of β-amyloid by magnetic resonance imaging and attenuation of β-amyloid induced cytotoxicity. ACS Chem Neurosci. 2013; 4:575–584. [PubMed: 23590250]
112. Liu LH, Dietsch H, Schurtenberger P, Yan M. Photoinitiated coupling of unmodified monosaccharides to iron oxide nanoparticles for sensing proteins and bacteria. Bioconjugate Chem. 2009; 20:1349–1355.
113. Jayawardena HSN, Jayawardana KW, Chen X, Yan M. Maltoheptaose promotes nanoparticle internalization by *Escherichia coli*. Chem Commun. 2013; 49:3034–3036.
114. Santra S, Wang KM, Tapec R, Tan WH. Development of novel dye-doped silica nanoparticles for biomarker application. J Biomed Opt. 2001; 6:160–166. [PubMed: 11375725]
115. Tan WH, Wang KM, He XX, Zhao XJ, Drake T, Wang L, Bagwe RP. Bionanotechnology based on silica nanoparticles. Med Res Rev. 2004; 24:621–638. [PubMed: 15224383]
116. Slowing II, Trewyn BG, Giri S, Lin VSY. Mesoporous silica nanoparticles for drug delivery and biosensing applications. Adv Funct Mater. 2007; 17:1225–1236.
117. Trewyn BG, Slowing II, Giri S, Chen HT, Lin VSY. Synthesis and functionalization of a mesoporous silica nanoparticle based on the sol–gel process and applications in controlled release. Acc Chem Res. 2007; 40:846–853. [PubMed: 17645305]
118. He QJ, Shi JL. MSN anti-cancer nanomedicines: Chemotherapy enhancement, overcoming of drug resistance, and metastasis inhibition. Adv Mater. 2013; 26:391–411. [PubMed: 24142549]
119. Zhao JS, Liu YF, Park HJ, Boggs JM, Basu A. Carbohydrate-coated fluorescent silica nanoparticles as probes for the galactose/3-sulfogalactose carbohydrate–carbohydrate interaction using model systems and cellular binding studies. Bioconjugate Chem. 2012; 23:1166–1173.
120. Peng JF, Wang KM, Tan WH, He XX, He CM, Wu P, Liu F. Identification of live liver cancer cells in a mixed cell system using galactose-conjugated fluorescent nanoparticles. Talanta. 2007; 71:833–840. [PubMed: 19071382]
121. Gary-Bobo M, Mir Y, Rouxel C, Brevet D, Basile I, Maynadier M, Vaillant O, Mongin O, Blanchard-Desce M, Morère A, et al. Mannose-functionalized mesoporous silica nanoparticles for efficient two-photon photodynamic therapy of solid tumors. Angew Chem Int Ed. 2011; 50:11425–11429.
122. Wang X, Ramström O, Yan M. Dye-doped silica nanoparticles as efficient labels for glycans. Chem Commun. 2011; 47:4261–4263.
123. Tong Q, Wang X, Wang H, Kubo T, Yan M. Fabrication of glyconanoparticle microarrays. Anal Chem. 2012; 84:3049–3052. [PubMed: 22385080]
124. Wang H, Tong Q, Yan M. Antifouling surfaces for proteins labeled with dye-doped silica nanoparticles. Anal Chem. 2012; 85:23–27. [PubMed: 23236953]
125. Barrientos AG, de la Fuente JM, Jiménez M, Solís D, Cañada FJ, Martín-Lomas M, Penadés S. Modulating glycosidase degradation and lectin recognition of gold glyconanoparticles. Carbohydr Res. 2009; 344:1474–1478. [PubMed: 19501815]
126. Houseman BT, Mrksich M. The role of ligand density in the enzymatic glycosylation of carbohydrates presented on self-assembled monolayers of alkanethiolates on gold. Angew Chem Int Ed. 1999; 38:782–785.
127. Eggeling C, Widengren J, Rigler R, Seidel CAM. Photobleaching of fluorescent dyes under conditions used for single-molecule detection: Evidence of two-step photolysis. Anal Chem. 1998; 70:2651–2659. [PubMed: 21644785]
128. Santra S, Dutta D, Moudgil BM. Functional dye-doped silica nanoparticles for bioimaging, diagnostics and therapeutics. Food Bioprod Process. 2005; 83:136–140.
129. Yan JL, Estévez MC, Smith JE, Wang KM, He XX, Wang L, Tan WH. Dye-doped nanoparticles for bioanalysis. Nano Today. 2007; 2:44–50.
130. Miletto I, Gilardino A, Zamburlin P, Dalmazzo S, Lovisolo D, Caputo G, Viscardi G, Martra G. Highly bright and photostable cyanine dye-doped silica nanoparticles for optical imaging: Photophysical characterization and cell tests. Dyes Pigm. 2010; 84:121–127.

131. Robinson A, Fang JM, Chou PT, Liao KW, Chu RM, Lee SJ. Probing lectin and sperm with carbohydrate-modified quantum dots. ChemBioChem. 2005; 6:1899–1905. [PubMed: 16149042]
132. Coulon J, Thouvenin I, Aldeek F, Balan L, Schneider R. Glycosylated quantum dots for the selective labelling of *Kluyveromyces bulgaricus* and *Saccharomyces cerevisiae yeast strains*. J Fluoresc. 2010; 20:591–597. [PubMed: 20058182]
133. Derfus AM, Chan WCW, Bhatia SN. Probing the cytotoxicity of semiconductor quantum dots. Nano Lett. 2003; 4:11–18.
134. Erogbogbo F, Yong KT, Roy I, Xu GX, Prasad PN, Swihart MT. Biocompatible luminescent silicon quantum dots for imaging of cancer cells. ACS Nano. 2008; 2:873–878. [PubMed: 19206483]
135. Cho SJ, Maysinger D, Jain M, Röder B, Hackbarth S, Winnik FM. Long-term exposure to CdTe quantum dots causes functional impairments in live cells. Langmuir. 2007; 23:1974–1980. [PubMed: 17279683]
136. Ahire JH, Chambrier I, Mueller A, Bao YP, Chao YM. Synthesis of D-mannose capped silicon nanoparticles and their Interactions with MCF-7 human breast cancerous cells. ACS Appl Mater Interfaces. 2013; 5:7384–7391. [PubMed: 23815685]
137. Wu CF, Chiu DT. Highly fluorescent semiconducting polymer dots for biology and medicine. Angew Chem Int Ed. 2014; 52:3086–3109.
138. Wu CF, Schneider T, Zeigler M, Yu JB, Schiro PG, Burnham DR, McNeill JD, Chiu DT. Bioconjugation of ultrabright semiconducting polymer dots for specific cellular targeting. J Am Chem Soc. 2010; 132:15410–15417. [PubMed: 20929226]
139. Kirchner C, Liedl T, Kudera S, Pellegrino T, Muñoz Javier A, Gaub HE, Stölzle S, Fertig N, Parak WJ. Cytotoxicity of colloidal CdSe and CdSe/ZnS nanoparticles. Nano Lett. 2004; 5:331–338. [PubMed: 15794621]
140. Lovrić J, Bazzi H, Cuie Y, Fortin GA, Winnik F, Maysinger D. Differences in subcellular distribution and toxicity of green and red emitting CdTe quantum dots. J Mol Med. 2005; 83:377–385. [PubMed: 15688234]
141. Lavigne JJ, Broughton DL, Wilson JN, Erdogan B, Bunz UHF. “Surfactochromic” conjugated polymers: Surfactant effects on sugar-substituted PPEs. Macromolecules. 2003; 36:7409–7412.
142. Disney MD, Zheng J, Swager TM, Seeberger PH. Detection of bacteria with carbohydrate-functionalized fluorescent polymers. J Am Chem Soc. 2004; 126:13343–13346. [PubMed: 15479090]
143. Pfaff A, Schallon A, Ruhland TM, Majewski AP, Schmalz H, Freitag R, Müller AHE. Magnetic and fluorescent glycopolymer hybrid nanoparticles for intranuclear optical imaging. Biomacromolecules. 2011; 12:3805–3811. [PubMed: 21875143]
144. Yung KT. Empirical models of transverse relaxation for spherical magnetic perturbers. Magn Reson Imaging. 2003; 21:451–463. [PubMed: 12878254]
145. El-Boubbou K, Zhu DC, Vasileiou C, Borhan B, Prosperi D, Li W, Huang XL. Magnetic glyconanoparticles: A tool to detect, differentiate, and unlock the glyco-codes of cancer via magnetic resonance imaging. J Am Chem Soc. 2010; 132:4490–4499. [PubMed: 20201530]
146. van Kasteren SI, Campbell SJ, Serres S, Anthony DC, Sibson NR, Davis BG. Glyconanoparticles allow pre-symptomatic in vivo imaging of brain disease. Proc Natl Acad Sci USA. 2009; 106:18–23. [PubMed: 19106304]
147. Debouttière PJ, Roux S, Vocanson F, Billotey C, Beuf O, Favre-Réguillon A, Lin Y, Pellet-Rostaing S, Lamartine R, Perriat P, et al. Design of gold nanoparticles for magnetic resonance imaging. Adv Funct Mater. 2006; 16:2330–2339.
148. Park JA, Reddy PAN, Kim HK, Kim IS, Kim GC, Chang YM, Kim TJ. Gold nanoparticles functionalised by Gd-complex of DTPA-bis(amide) conjugate of glutathione as an MRI contrast agent. Bioorg Med Chem Lett. 2008; 18:6135–6137. [PubMed: 18938074]
149. Li Y, Beija M, Laurent S, Elst LV, Muller RN, Duong HTT, Lowe AB, Davis TP, Boyer C. Macromolecular ligands for gadolinium MRI contrast agents. Macromolecules. 2012; 45:4196–4204.

150. Sun M, Zhang HY, Liu BW, Liu Y. Construction of a supramolecular polymer by bridged bis(permethyl-β-cyclodextrin) s with porphyrins and its highly efficient magnetic resonance imaging. Macromolecules. 2013; 46:4268–4275.

151. Marradi M, Alcántara D, de la Fuente JM, García-Martín ML, Cerdán S, Penadés S. Paramagnetic Gd-based gold glyconanoparticles as probes for MRI: Tuning relaxivities with sugars. Chem Commun. 2009:3922–3924.

152. Pelizzari CA, Chen GTY, Spelbring DR, Weichselbaum RR, Chen CT. Accurate three-dimensional registration of CT, PET, and/or MR images of the brain. J Comput Assist Tomo. 1989; 13:20–26.

153. Beyer T, Townsend DW, Brun T, Kinahan PE, Charron M, Roddy R, Jerin J, Young J, Byars L, Nutt R. A combined PET/CT scanner for clinical oncology. J Nucl Med. 2000; 41:1369–1379. [PubMed: 10945530]

154. Kapoor V, McCook BM, Torok FS. An Introduction to PET–CT imaging. Radiographics. 2004; 24:523–543. [PubMed: 15026598]

155. Yang Z, Zheng SY, Harrison WJ, Harder J, Wen XX, Gelovani JG, Qiao A, Li C. Long-circulating near-infrared fluorescence core-cross-linked polymeric micelles: Synthesis, characterization, and dual nuclear/optical imaging. Biomacromolecules. 2007; 8:3422–3428. [PubMed: 17958440]

156. Zhu H, Zhao J, Lin XF, Hong Y, Li C, Yang Z. Design, synthesis and evaluation of dual-modality glyconanoparticles for tumor imaging. Molecules. 2013; 18:6425–6438. [PubMed: 23722731]

157. Gu LR, Elkin T, Jiang XP, Li HP, Lin Y, Qu LW, Tzeng TRJ, Joseph R, Sun YP. Single-walled carbon nanotubes displaying multivalent ligands for capturing pathogens. Chem Commun. 2005:874–876.

158. Gu LR, Luo PG, Wang HF, Meziani MJ, Lin Y, Veca LM, Cao L, Lu FS, Wang X, Quinn RA, et al. Single-walled carbon nanotube as a unique scaffold for the multivalent display of sugars. Biomacromolecules. 2008; 9:2408–2418. [PubMed: 18712920]

159. Yang Y, Zhao YT, Yan TT, Yu M, Sha YL, Zhao ZH, Li ZJ. Design and fabrication of multivalent Gal-containing quantum dots and study of its interactions with asialoglycoprotein receptor (ASGP-R). Tetrahedron Lett. 2010; 51:4182–4185.

160. Cai XJ, Li XH, Liu YW, Wu GN, Zhao YC, Chen F, Gu ZW. Galactose decorated acid-labile nanoparticles encapsulating quantum dots for enhanced cellular uptake and subcellular localization. Pharm Res. 2012; 29:2167–2179. [PubMed: 22477071]

161. Osaki F, Kanamori T, Sando S, Sera T, Aoyama Y. A quantum dot conjugated sugar ball and its cellular uptake. On the size effects of endocytosis in the subviral region. J Am Chem Soc. 2004; 126:6520–6521. [PubMed: 15161257]

162. Ohyanagi T, Nagahori N, Shimawaki K, Hinou H, Yamashita T, Sasaki A, Jin T, Iwanaga T, Kinjo M, Nishimura SI. Importance of sialic acid residues illuminated by live animal imaging using phosphorylcholine self-assembled monolayer-coated quantum dots. J Am Chem Soc. 2011; 133:12507–12517. [PubMed: 21740000]

163. Martínez-Ávila O, Hijazi K, Marradi M, Clavel C, Campion C, Kelly C, Penadés S. Gold manno-glyconanoparticles: Multivalent systems to block HIV-1 gp120 binding to the lectin DC-SIGN. Chem—Eur J. 2009; 15:9874–9888. [PubMed: 19681073]

164. Martínez-Ávila O, Bedoya LM, Marradi M, Clavel C, Alcamí J, Penadés S. Multivalent manno-glyconanoparticles inhibit DC-SIGN-mediated HIV-1 trans-infection of human T cells. ChemBioChem. 2009; 10:1806–1809. [PubMed: 19565596]

165. Luczkowiak J, Muñoz A, Sánchez-Navarro M, Ribeiro-Viana R, Ginieis A, Illescas BM, Martín N, Delgado R, Rojo J. Glycofullerenes inhibit viral infection. Biomacromolecules. 2013; 14:431–437. [PubMed: 23281578]

166. Dougherty TJ, Dougherty TJ, Gomer CJ, Jori G, Kessel D, Korbelik M, Moan J, Peng Q. Photodynamic therapy. J Natl Cancer Inst. 1998; 90:889–905. [PubMed: 9637138]

167. Brevet D, Gary-Bobo M, Raehm L, Richeter S, Hocine O, Amro K, Loock B, Couleaud P, Frochot C, Morère A, et al. Mannose-targeted mesoporous silica nanoparticles for photodynamic therapy. Chem Commun. 2009:1475–1477.

168. Perrier M, Gary-Bobo M, Lartigue L, Brevet D, Morère A, Garcia M, Maillard P, Raehm L, Guari Y, Larionova J, et al. Mannose-functionalized porous silica-coated magnetic nanoparticles for two-photon imaging or PDT of cancer cells. J Nanopart Res. 2013; 15:1–17.

169. Laurent S, Dutz S, Häfeli UO, Mahmoudi M. Magnetic fluid hyperthermia: Focus on superparamagnetic iron oxide nanoparticles. Adv Colloid Interface Sci. 2011; 166:8–23. [PubMed: 21601820]

170. Deatsch AE, Evans BA. Heating efficiency in magnetic nanoparticle hyperthermia. J Magn Magn Mater. 2014; 354:163–172.

171. Salunkhe AB, Khot VM, Pawar SH. Magnetic hyperthermia with magnetic nanoparticles: A status review. Curr Top Med Chem. 2014; 14:572–594. [PubMed: 24444167]

172. Mornet S, Vasseur S, Grasset F, Duguet E. Magnetic nanoparticle design for medical diagnosis and therapy. J Mater Chem. 2004; 14:2161–2175.

173. Hergt R, Dutz S, Müller R, Zeisberger M. Magnetic particle hyperthermia: Nanoparticle magnetism and materials development for cancer therapy. J Phys: Condens Matter. 2006; 18:S2919.

174. Thiesen B, Jordan A. Clinical applications of magnetic nanoparticles for hyperthermia. Int J Hyperthermia. 2008; 24:467–474. [PubMed: 18608593]

175. Shubayev VI, Pisanic TR II, Jin S. Magnetic nanoparticles for theragnostics. Adv Drug Delivery Rev. 2009; 61:467–477.

176. Kumar CS, Mohammad F. Magnetic nanomaterials for hyperthermia-based therapy and controlled drug delivery. Adv Drug Delivery Rev. 2011; 63:789–808.

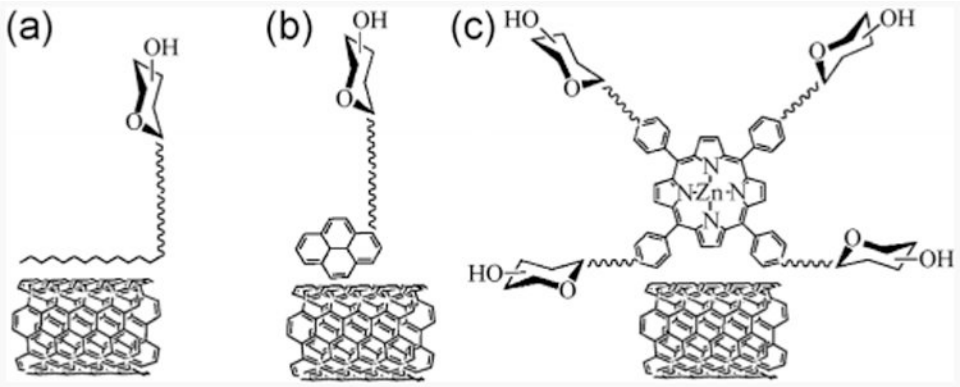

Figure 1.

Carbohydrate immobilization through non-covalent interactions via (a) lipids, (b) polyaromatic hydrocarbons and (c) porphyrins.

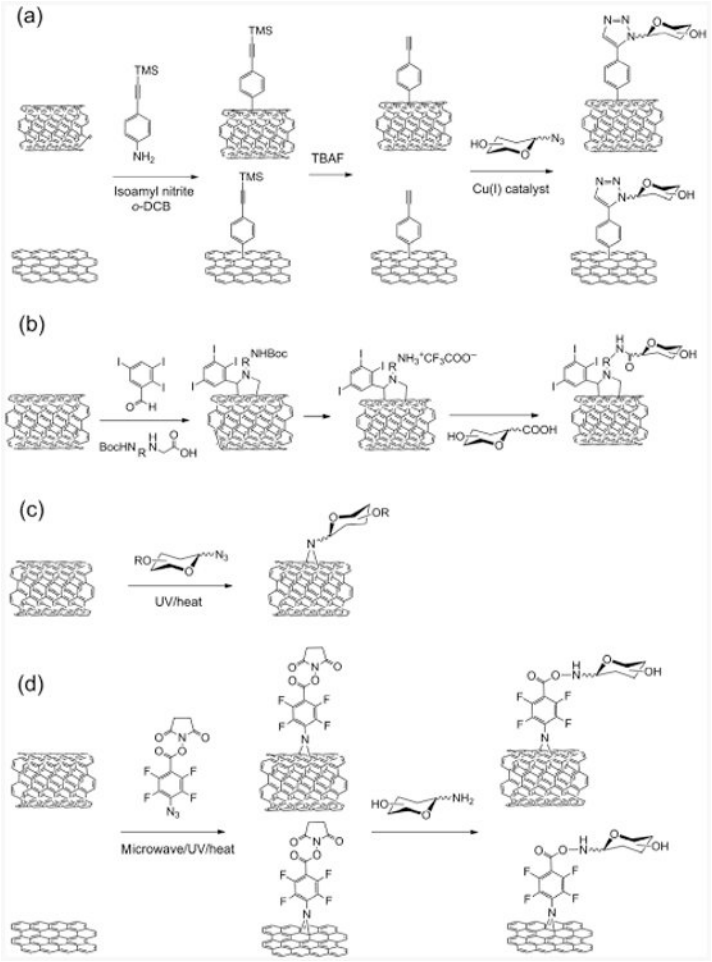

Figure 2.

Methods for direct functionalization of pristine CNTs or graphene using (a), aryl diazonium salt, (b) azomethine ylide, (c) alkyl azide, and (d) PFPA.

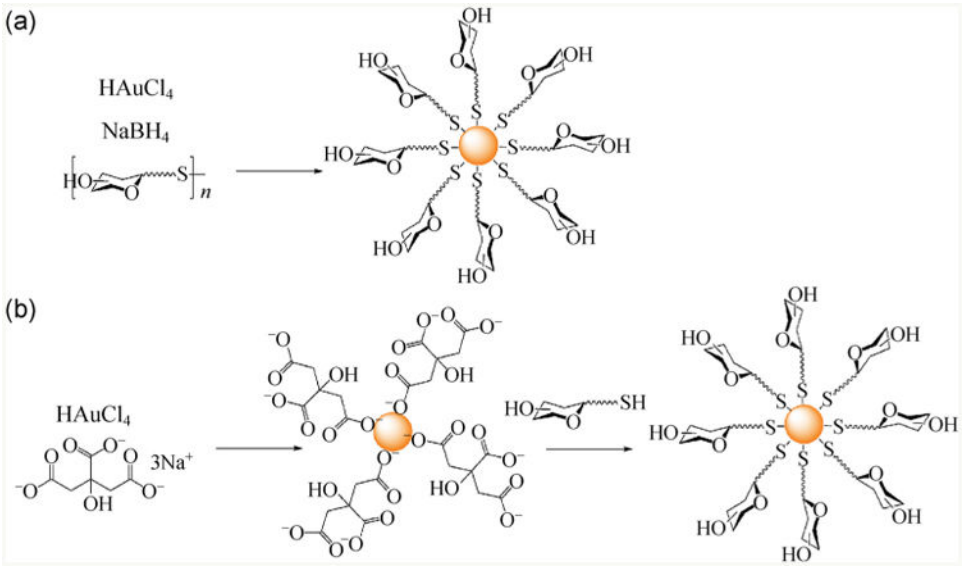

Figure 3.
Grafting carbohydrates onto AuNPs through (a) one-pot and (b) two-step process.

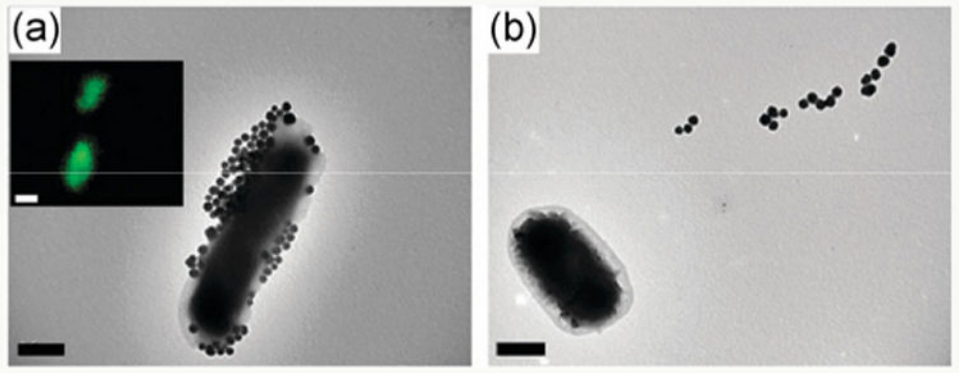

Figure 4.

Fluorescence and TEM image of Man-FSNPs interacting with (a) *E. coli* ORN 178 and (b) *E. coli* ORN 208. (Copyright Royal Society of Chemistry. Reproduced from Ref. [122] with permission.)

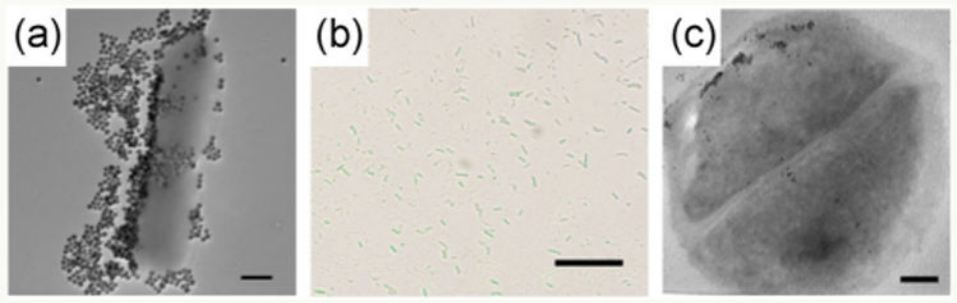

Figure 5.

(a) TEM image of maltoheptaose-conjugated SNPs treated with *E. coli* ATCC 33456 (scale bar: 500 nm). (b) Overlay of confocal laser scanning microscopy image and bright field image (scale bar: 10 μm). The SNPs were doped with FITC. (c) TEM thin section image of maltoheptaose-conjugated iron oxide nanoparticles treated with *E. coli* ATCC 33456 (scale bar: 100 nm). (Copyright Royal Society of Chemistry. Reproduced from Ref. [113] with permission.)

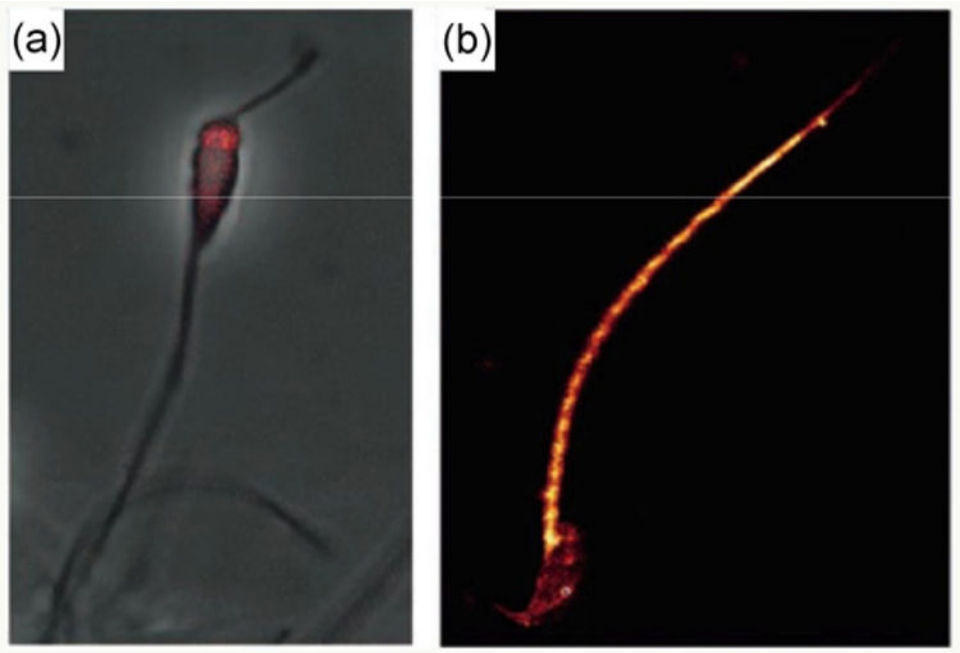

Figure 6.

(a) Confocal fluorescence microscopy images of sea-urchin sperm selectively labeled on the head by GlcNAc-QDs (scale bar = 20 μm). (b) Mouse sperm labeled with Man-QDs. (Copyright Wiley-VCH. Reproduced from Ref. [131] with permission.)

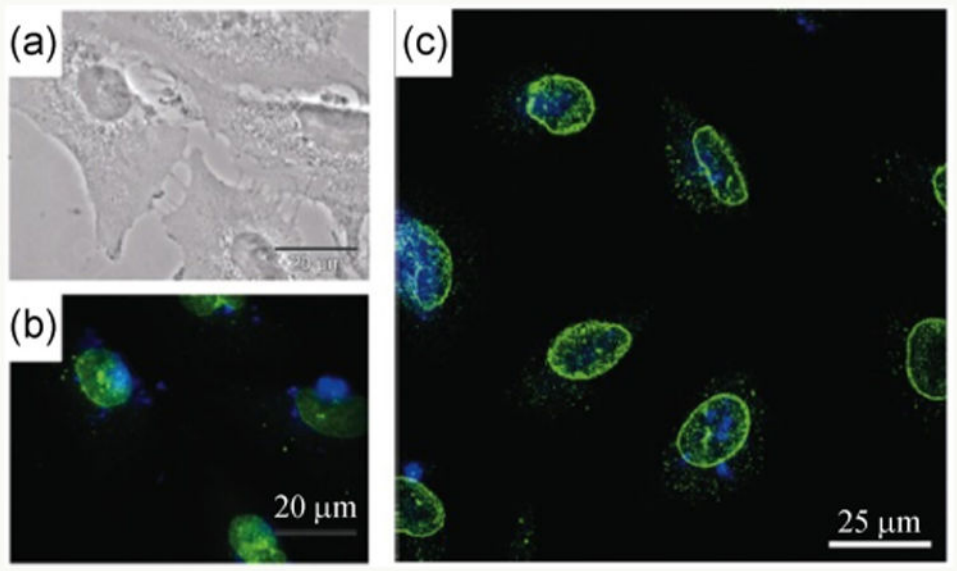

Figure 7.

Laser scanning confocal image of galactose- and pyrene-grafted poly(methacrylate) copolymers coated silica-protected MNPs with A549 cells (a) transmission image (scale bar: 20 μm), (b) epifluorescence microscopy image, and (c) confocal microscopy images. The green emission is from the nuclei stain antiNUP98-FITC and the blue emission is from glycopolymer coated nanoparticles. (Copyright American Chemical Society. Reproduced from Ref. [143] with permission.)

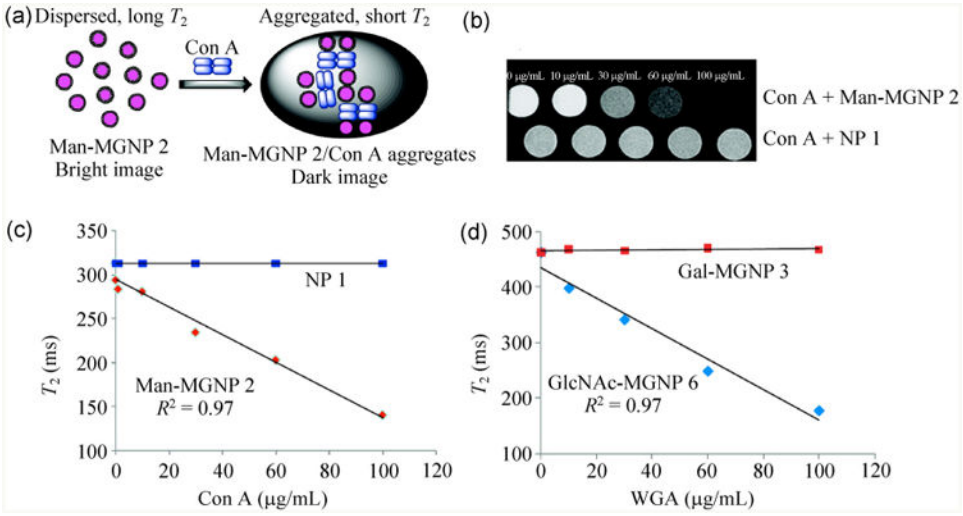

Figure 8.

(a) Aggregation of Man-MGNPs in the presence of Con A. (b) T_2-weighted MRI images of Con A treated with Man-MGNPs and unfunctionalized NPs. (c) T_2 vs. Con A concentration for Man-MGNPs and NPs. (d) T_2 vs. WGA concentration for GlcNAc-MGNPs and Gal-MGNPs. (Copyright American Chemical Society. Reproduced from Ref. [145] with permission.)

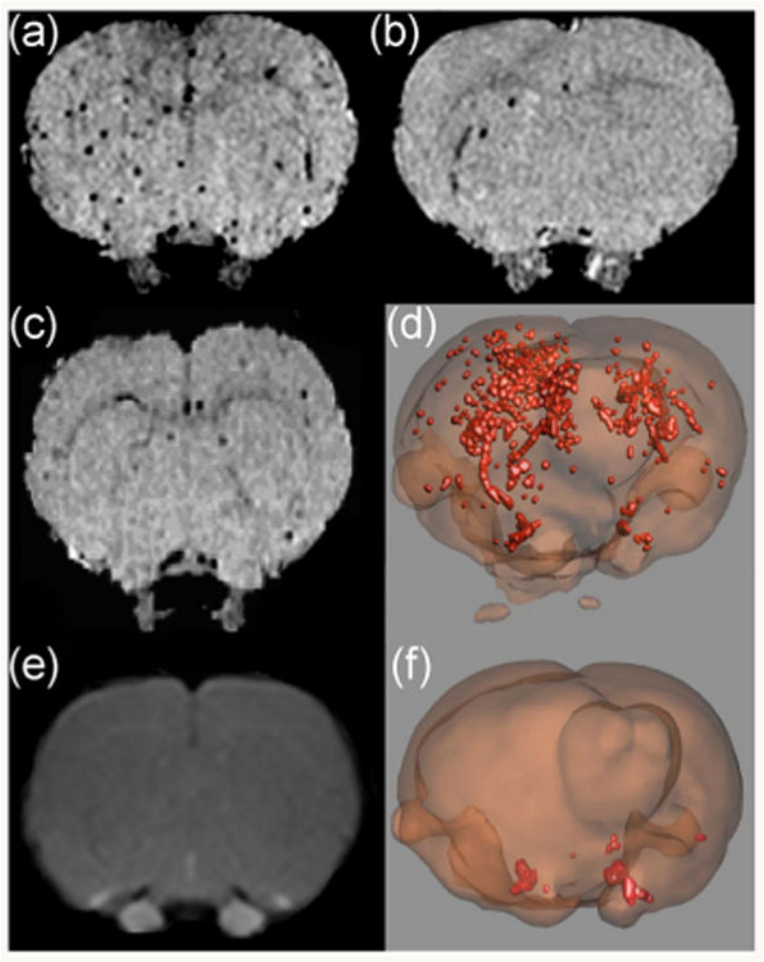

Figure 9.

In vivo MRI and 3D images of sLe^x-MNPs in the brain. (a) and (b) MRI images after intracerebral injection of 100 and 10 ng interleukin-1β followed by sLe^x-MNPs. (c) MRI image after injection of 100 ng interleukin-1β followed by MNPs. (d) 3D image of (b). (e) MRI image showing a lack of blood-brain barrier breakdown after 5.5 h incubation. (f) 3D image after sterile saline injection followed by sLe^x-MNPs, showing low binding. (Copyright Proceedings of the National Academy of Science. Reproduced from Ref. [146] with permission.)

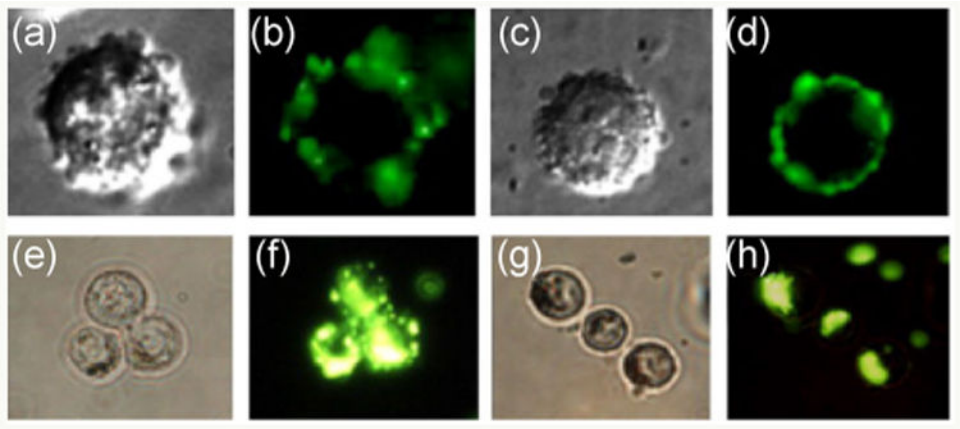

Figure 10.

HepG2 cells incubated for 30 min with Lac-QDs (a) and (b) and Gal-QDs (c) and (d), HepG2 cells incubated for 4 h with Lac-QDs (e) and (f) and Gal-QDs (g) and (h). (Copyright Elsevier. Reproduced from Ref. [159] with permission.)

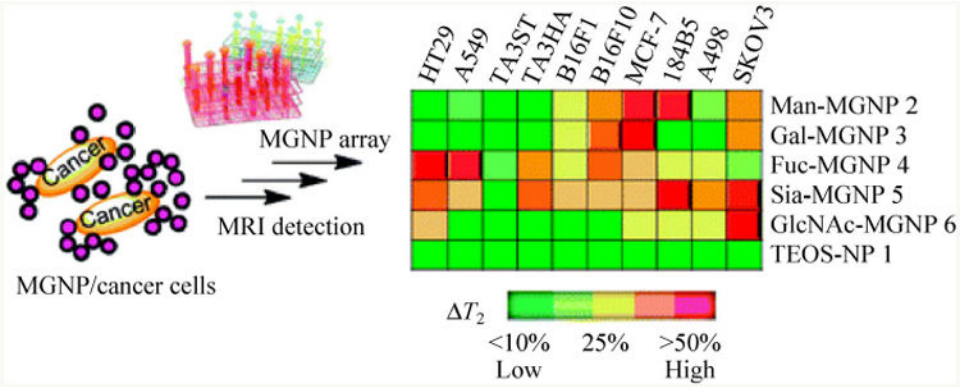

Figure 11.

Response patterns of cancer cell array interacting with glyco-MNPs. (Copyright American Chemical Society. Reproduced from Ref. [145] with permission.)

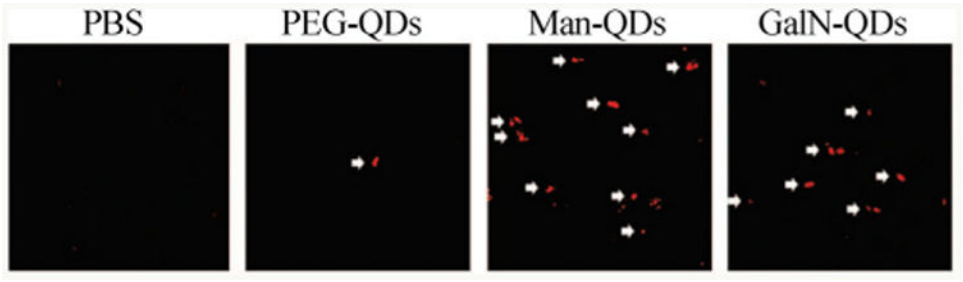

Figure 12.

Paraffin sections of mice livers after injection of PBS, PEG-QDs, Man-QDs, GalN-QDs (red is from QDs and white is the arrow that indicates the QDs). (Copyright American Chemical Society. Reproduced from Ref. [98] with permission.)

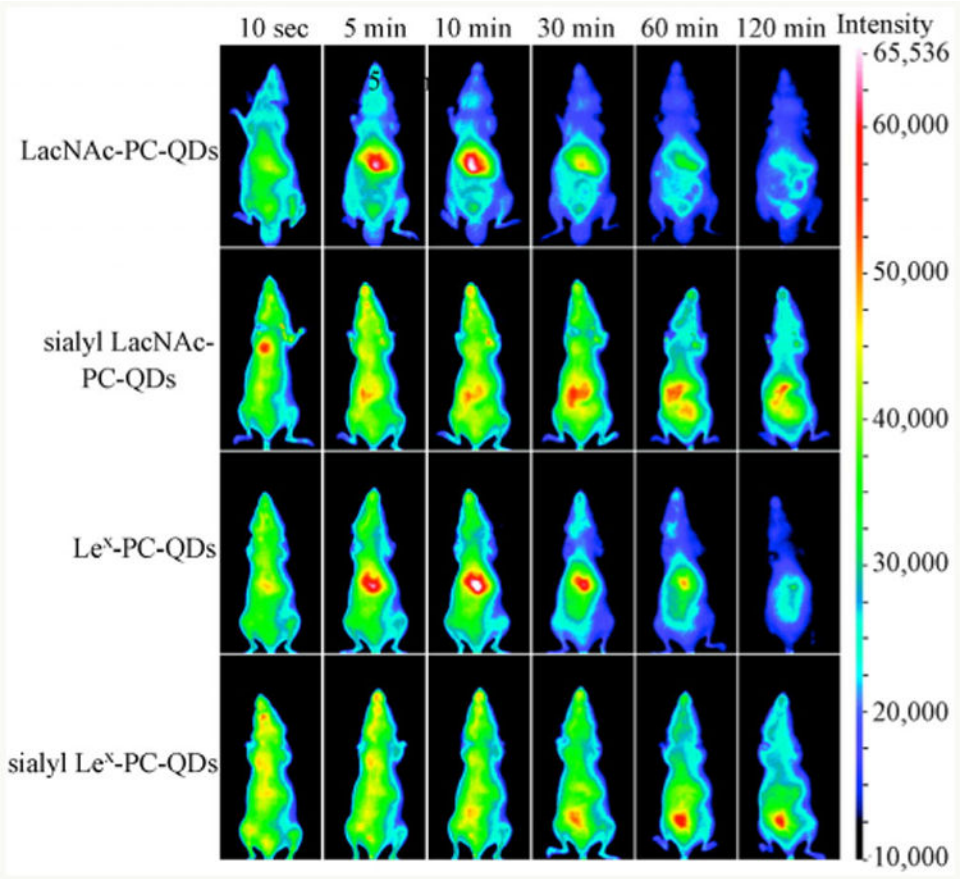

Figure 13.

Live animal imaging of glyco-QDs carrying Lewis antigen-related oligosaccharides (PC = undecylphosphorylcholine). (Copyright American Chemical Society. Reproduced from Ref. [162] with permission.)

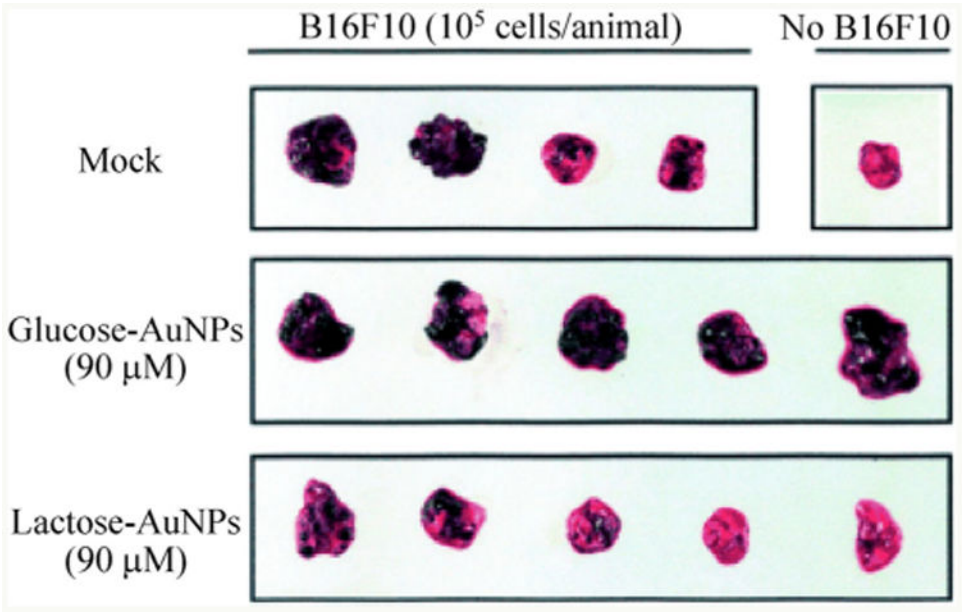

Figure 14.
B16F10 melanoma cell treated C57/B16 mice lung with lactose-AuNPs and glucose-AuNPs. (Copyright Wiley-VCH. Reproduced from Ref. [84] with permission.)